ELSEVIER

In Collaboration with
the Netherlands Institute for Sea Research

JOURNAL OF SEA RESEARCH

Journal of Sea Research 38 (1997) 249–274

The effects of river input on the ecosystem dynamics in the continental coastal zone of the North Sea using ERSEM

Hermann J. Lenhart [a,*], Günther Radach [a], Piet Ruardij [b]

[a] *Institut für Meereskunde der Universität Hamburg, Troplowitzstrasse 7, D-22529 Hamburg, Germany*
[b] *Netherlands Institute for Sea Research, PO Box 59, 1790 AB Den Burg, The Netherlands*

Received 3 February 1997; accepted 23 June 1997

Abstract

The general characteristics of the continental coastal zone, with nutrient concentrations, primary production and biomass high near the coast but decreasing with distance from the coast, are simulated by a box-refined version of the ecosystem model ERSEM. Aggregated model results compared to the literature as well as to two different three-dimensional models show a good agreement in the coastal region. The dynamical interactions as simulated by the ecosystem model are presented in the form of N/P ratios, the limitation by various nutrients and changes in the pathways of the flow of matter in the boxes; e.g. while the silicate limitation stops the spring bloom offshore, near the coast it is terminated by zooplankton grazing. When the river load was reduced by 50%, the largest effect was observed in the coastal boxes with 15% reduction of the net primary production. The discharges of the major rivers hardly affect the central North Sea, but lead to significant changes in nutrient limitations and mass flows in the coastal area. The realistic forcing, which was adopted for this setup, allows a higher net primary production in the southern North Sea in 1989 than in 1988, even though the nutrient river loads in 1989 were lower. The reason appears to be a higher solar energy input in 1989, by about 10 W m^{-2} d^{-1}, compared to 1988.

Keywords: ecosystem model; North Sea; eutrophication; nutrient budgets; nutrient reduction scenarios; ERSEM

1. Introduction

The continental coastal region of the southern North Sea is strongly influenced by the discharge of the rivers Rhine, Meuse and Elbe. The freshwater supply by these rivers leads to strong salinity gradients perpendicular to the coast. The region influenced by freshwater off the Dutch coast extends 70 km offshore near the mouth of the Rhine and elsewhere 30 km (Klein and Van Buuren, 1992). Along with the freshwater, high nutrient loads are supplied by the rivers, which lead to eutrophication problems in the coastal region. High nutrient contents in the water in combination with high primary production or large biomasses are biochemical properties characteristic of the continental coastal zone, e.g. Peeters and Peperzak (1990) found an average annual primary production of about 325 g C m^{-2} in the 1988 to 1990 period.

The ecosystem model ERSEM (European Regional Seas Ecosystem Model) was developed to simulate the ecosystem dynamics of the North Sea. The model simulates the annual cycles of carbon,

* Corresponding author. Tel.: +49 (40) 4123 5743; Fax: +49 (40) 560 5724; E-mail: lenhart@ifm.uni-hamburg.de

1385-1101/97/$17.00
PII S1385-1101(97)00049-X

nitrogen, phosphorus and silicon in the pelagic and benthic food webs of the North Sea. The box model combines hydrodynamical and ecological processes into one model with the same resolution in space and time. The model is forced by daily values of irradiance, temperature, suspended matter concentration and transport data for advection and diffusion. In the first phase of the ERSEM project a 15-box setup (the so-called setup ND15) was used. Results from this setup indicated that the spatial resolution of the model was too coarse. Radach and Lenhart (1995) suggested that improvements of the model results compared to observations can be obtained by refining the box structure to reduce the artificial diffusivity and to better resolve spatial gradients along the continental coast. Therefore in the second phase of the project a $1° \times 1°$ model setup of the North Sea was created as new standard model, containing 130 boxes in total (the so-called setup ND130).

To simulate the full scale of the characteristic ecosystem properties with an increased resolution in the continental coastal region, ERSEM was further adapted in its structural setup by reducing the size of the boxes. This box setup of ERSEM called COCOA (continental coastal application) has 138 boxes in total, allowing a focus on the nutrient dynamics of the continental coastal waters which are characterised by high N/P ratios near the coast. Therefore COCOA shows a higher resolution in the coastal area than the ND130, while the boxes of the central and northern North Sea are larger.

The focus of this paper is on the dynamical interactions as simulated by ERSEM to describe different ecosystem dynamics with distance from the coast, the effect of a reduction of the riverine nutrient loads, and the effect of excluding atmospheric loads and particulate organic matter as part of the river loads.

2. Model setup

The biological part of the model (ERSEM version 11) consists of an interlinked set of modules, describing the biological and chemical interactions between the state variables, which can be coupled to each of the three model setups for which specific physical forcing is applied, depending on the box structure. A general description of the model is given by Baretta et al. (1995). The primary production module in ERSEM, consisting of diatoms and flagellates, was first presented by Varela et al. (1995). The present version 11 includes as primary producers four phytoplankton groups, i.e. diatoms, flagellates, picophytoplankton and inedibles, as described by Ebenhöh et al. (1997) and Baretta-Bekker et al. (1997). The secondary producers consist of heterotrophic flagellates, microzooplankton (Baretta-Bekker et al., 1995) and mesozooplankton (Broekhuizen et al., 1995). Within the microbial food web the bacteria and the particulate organic matter are simulated as state variables while the fluxes through dissolved organic matter are parameterised (Baretta-Bekker et al., 1995, 1998). In the sediment the biological dynamics of the benthic secondary producers is included (Blackford, 1997) as well as the breakdown of detrital material in the form of benthic nutrient regeneration (Ruardij and Van Raaphorst, 1995).

For the standard simulation the years 1988 and 1989 were chosen, since a large set of validation data for these two years is available from the Natural Environment Research Council (NERC) North Sea Programme (Howarth et al., 1994) and from other sources. To represent the ecosystem dynamics in the coastal region with its highly variable conditions the relevant information on the morphology has been provided and the transport processes are parameterised on the scale of the refined box setup of COCOA. Apart from the transport forcing, additional realistic forcing is provided for the years 1988 and 1989 to the COCOA model setup in the form of time series for radiation, suspended matter concentration and inorganic and organic river input. For the atmospheric nitrogen input a constant load is applied to the entire model domain as a first approximation of this additional external source. With the introduction of the atmospheric input the ecosystem model is an extension of the ERSEM version 11.

2.1. Spatial characteristics of the COCOA setup

Even though the continental coastal region is the main focus of this application, the model domain covers the whole North Sea. This avoids an open boundary in the vicinity of the area of interest. The model area now extends into the Skagerrak to resolve problems with the recirculation of the

Jutland current within this region. The aim was to have a Baltic boundary which represents an area where the Baltic outflow is dominant and therefore a realistic boundary condition can be prescribed. This setup also allows for a comparison with the setup ND15 of ERSEM by aggregation of the model results in relation to the box volume. This is useful, since the setup ND15 is related to the division of the North Sea into the ICES-boxes (ICES, 1983), which are often used to present data aggregated from measurements or model results (Anonymous, 1995; Moll, 1995; Lenhart and Pohlmann, 1997).

In Fig. 1a the surface boxes of the model area of COCOA are presented, covering in total an area of 577 620 km^2 and a volume of 51 047 km^3. The northern and central parts of the North Sea are divided into $1° \times 2°$ boxes, which is equivalent to 5×6 grid points of the hydrodynamical model grid of HAMSOM (Backhaus, 1985). For resolving the horizontal gradients in the coastal areas the division was reduced to boxes of $0.5° \times 1°$ degree, which were adjusted to the actual coastline, if necessary. In this way, the model is finely resolved in the coastal area, but also represents the central and northern North Sea at a resolution which is still much higher than the setup ND15 of ERSEM (Lenhart et al., 1995).

The central and northern boxes of the ND15 version of ERSEM were vertically separated in order to represent the biological processes acting within the euphotic zone. Such a vertical division also had to be introduced in the COCOA setup. Since the hydrodynamical model (Pohlmann, 1991, 1996a,b) provides information on salinity and temperature, the concept of potential energy was used to define stratification within a box (Simpson et al., 1977; Reid et al., 1988; Lenhart and Pohlmann, 1997). The idea was to achieve a vertical box separation in a consistent way from the same model as the one from which the advective and diffusive transport information stems. In Fig. 1b the boxes which have a vertical separation are presented with the box numbers of the lower boxes. One can clearly see the lack of stratification near the Orkneys (boxes 25–27) and in the region of the Dogger Bank (boxes 52–54) while the Skagerrak region (boxes 13 and 14) reflects the strongly haline stratification. For comparison, the 15-box version ND15 of ERSEM is presented in Fig. 1c.

2.2. Transport adaptation

In ERSEM the physical transport of pelagic abiotic and biotic substances is based on physical flow fields simulated by the three-dimensional general circulation model for the North Sea by Pohlmann (1991, 1996a,b). This model is an extension of the general shelf sea circulation model HAMSOM (Hamburg Shelf Ocean Model) developed by Backhaus (1985), based on the primitive shallow water equations. Including temperature as a prognostic state variable, the Pohlmann model is a three-dimensional baroclinic model. The circulation model was driven by three-hourly wind stress and air pressure distributions and by observed sea surface temperature. Details of the model setup and the results are described by Backhaus (1985), Backhaus and Hainbucher (1987) and by Pohlmann (1991, 1996a,b). For further information on the adaptation of flow fields of the three-dimensional model to the ERSEM box model see Lenhart et al. (1995) and Lenhart and Pohlmann (1997).

For the setup ND15 of ERSEM the correctness of the transport of substances was judged by setting up a scenario in which the results from the box model were compared with the fully resolved three-dimensional dispersion model (Lenhart and Pohlmann, 1997). Both models were run with the same hydrodynamical forcing and the same time series of freshwater discharge as was used as conservative tracer, released from a point source. With the same scenario the COCOA model was tested against the diffusion model. Fig. 2 shows time series of the amount of tracer substance integrated over all boxes of the model domain and summed for every day as percentage of freshwater related to the North Sea volume. The bold line (Total) represents the total amount of tracer introduced into the model area while the wiggly thin line represents the contents of the tracer in the dispersion model. The latter becomes lower than the total amount when some of the tracer substance leaves the model domain over the external boundaries in the dispersion model. The lines referred to as Net and Net + HDif show the results of the two different parameterisations of the transport within the COCOA setup of ERSEM. The first (Net) uses only the net transport over the box boundaries, and the second (Net + HD-

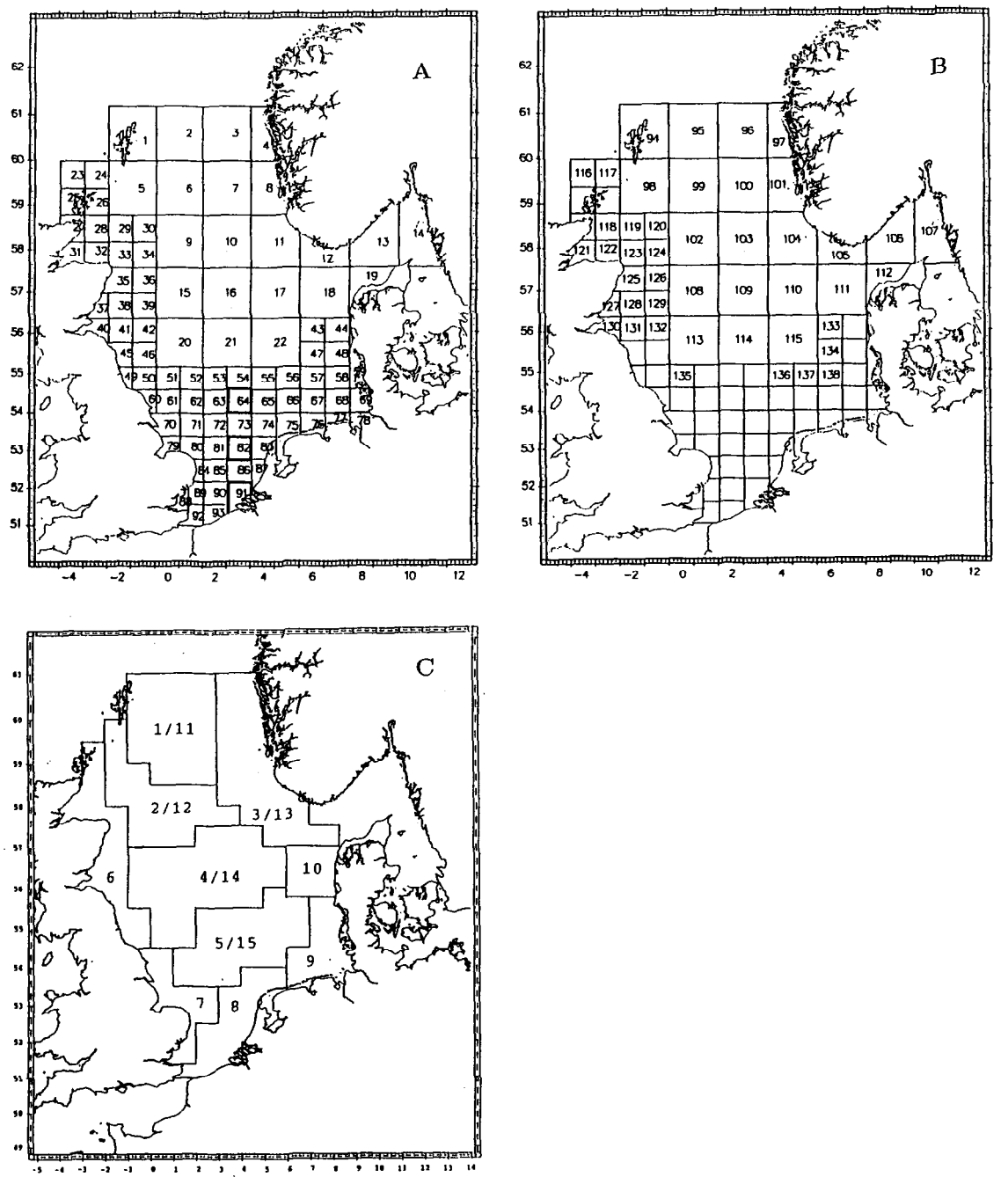

Fig. 1. (a) The surface boxes of the model area of COCOA. The selected boxes 91, 82 and 64 are outlined. (b) The lower boxes of the model area of COCOA. (c) The boxes of the model area of the setup ND15 of ERSEM.

if) uses the net transport plus a horizontal diffusion, applying twice the HAMSOM grid as horizontal diffusive length scale. Because the net transport constantly overestimates the amount of tracer in the model area, the net transport plus horizontal diffusion is the appropriate representation of the transport

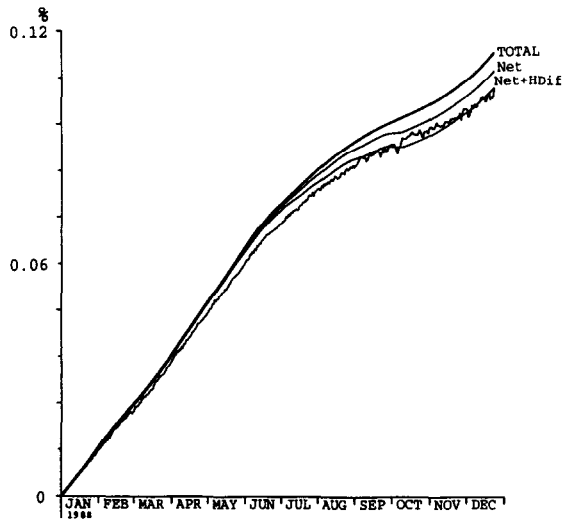

Fig. 2. The freshwater tracer as simulated by the three-dimensional dispersion model versus the COCOA setup of ERSEM, both using the same physical forcing. Cumulative time series as percentage of freshwater tracer in relation to the North Sea volume for: (*Total*) the total amount of tracer in the system, ERSEM parameterisations using: (*Net*) net advective transport only, (*Net + HDif*) net transport plus horizontal diffusion and (thin line) the results of the integrated three-dimensional dispersion model.

which was then implemented in the box model COCOA.

2.3. Radiational forcing and attenuation

A synthetic time series of daily solar radiation generated by the MOCADOB model (Pätsch, 1994) is used for each surface box of the COCOA model. These values are calculated using monthly frequency distributions of observed cloudiness. The distributions are given in 2° × 1° cells over the North Sea.

To include the effect of spatial and temporal variations on the light attenuation by suspended matter (SPM), box concentrations of SPM were calculated from the output of a suspended matter model (Puls and Sündermann, 1990; Pohlmann and Puls, 1994). The suspended matter concentrations are derived as volume-weighted daily mean values for each box. As the observational data from the NERC North Sea Programme differed greatly from the simulated SPM values, the daily mean values calculated from the simulation results were re-calibrated with the observational data as reference level.

2.4. River loads

For the rivers Elbe, Weser, Ems, Lake IJssel (inlets Kornwerderzand and Den Oever), Noordzeekanaal, Rhine, Meuse and Scheldt, time series of daily estimates of the dissolved inorganic and organic nutrient loads are prescribed based on a study by Lenhart et al. (1996). The estimates for the dissolved nutrients in the model consist of phosphate, nitrate, ammonium and silicate. The particulate organic loads from these rivers enter the model as contributions to the state variable detritus, separated into phosphorus, nitrogen and silicon. For all other rivers the forcing was the same as for the setup ND15, using monthly mean load estimates provided by the North Sea Task Force (Anonymous, 1992), as described by Radach and Lenhart (1995).

In Fig. 3 the time series of estimated phosphate loads of the years 1987 to 1990 are shown for five rivers entering the North Sea. These are subsets from the study by Lenhart et al. (1996), where time series of daily river loads were calculated from 1977 until 1994. Strong differences can be observed in the total nutrient load as well as in the interannual variation for each river, with the highest loads occurring in spring. The major contributions come from the Rhine with phosphate loads of 16.8×10^6 kg a^{-1} in 1988 and 12.6×10^6 kg a^{-1} in 1989 and from the Meuse with 5.2×10^6 kg a^{-1} in 1988 and 2.0×10^6 kg a^{-1} in 1989. All load estimates decrease between 1977 and 1994 (Lenhart et al., 1996). Therefore the values of 1988 and 1989 are at the lower end of the annual estimates, with a maximum of 21.0×10^6 kg a^{-1} and a minimum of 6.7×10^6 kg a^{-1} for the Rhine and between 10.6×10^6 kg a^{-1} and 1.2×10^6 kg a^{-1} for the Meuse. The loads of the Elbe and the Weser are much lower (note the different scales in Fig. 3) than the ones for the Rhine and Meuse, but the general tendency is the same. While the Rhine and the Meuse enter box 91, Elbe and Weser discharge into box 78 and the Ems into box 76 of the COCOA setup.

2.5. Atmospheric loads

The atmospheric input of nitrogen to the North Sea is considerable and cannot be neglected. However, the data for the atmospheric loads are sparse and provide mainly overall loads for the North Sea

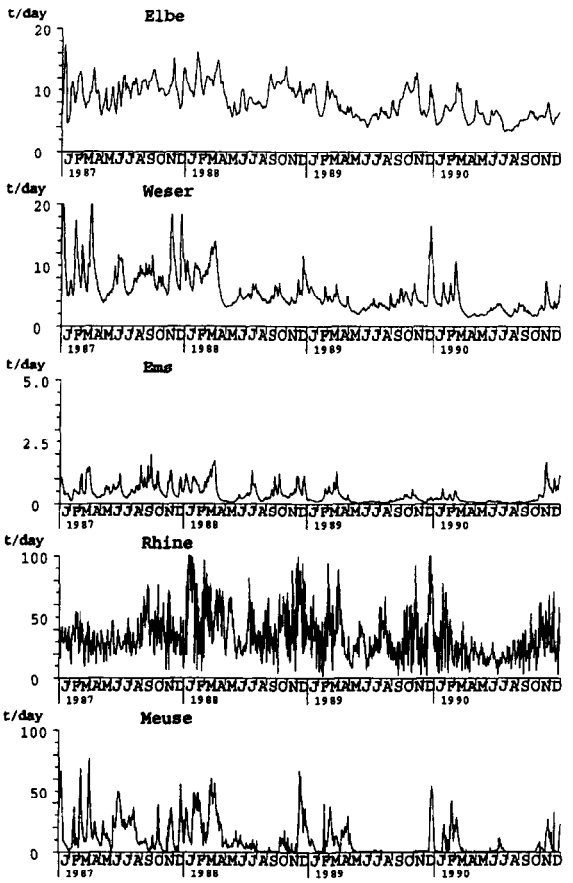

Fig. 3. Time series of calculated daily phosphate river loads for the years 1987 to 1990 (Lenhart et al., 1996) for the rivers Elbe, Weser, Ems, Rhine and Meuse entering the North Sea in 10^3 kg d^{-1} phosphate (note different scales on the y-axis).

as a whole or selected parts, e.g., the German Bight (Beddig et al., 1995). For this study, figures given in the Quality Status Report by the North Sea Task Force (Anonymous, 1995) have been used. Here a minimum value of 330×10^6 kg a^{-1} and a maximum value of 520×10^6 kg a^{-1} are given as an estimate of the total atmospheric nitrogen load for the North Sea. Selecting the maximum values as reference value and assuming 525 000 km^2 as the area for the North Sea, about 990 kg N km^{-2} a^{-1} or 70.74 mmol N m^{-2} a^{-1} as atmospheric nitrogen load has been introduced. This overall load is equally divided between the two ERSEM state variables nitrate and ammonium. In a study by Rendell et al. (1993), where detailed measurements were provided for the southern North Sea, the total nitrogen input was estimated to be 412×10^6 kg a^{-1}. About 95% of this input consists of nitrate and ammonium. By extrapolating from the detailed atmospheric load estimates for the different nitrogen species for the southern North Sea to the overall input to the whole North Sea, loads of about 244.3×10^6 kg for nitrate and 153.4×10^6 kg a^{-1} for ammonium have been calculated. The estimates applied as forcing in COCOA are close to the calculations for nitrate but they are higher for the ammonium load. In the calculation for the German Bight, Beddig et al. (1995) used the same partitioning of the total nitrogen load into nitrate and ammonium load as was done for COCOA. With the extended model area of 577 620 km^2 for the COCOA setup, which covers the North Sea plus the Skagerrak, the annual load is 286×10^6 kg N a^{-1} both for nitrate and ammonium.

2.6. Initial and boundary values

The initialisation for the standard run is obtained by running the model for 30 years with repeated forcing to obtain repeating annual cycles. The values after 30 years on 1 January are then used as initialisation for all state variables in the standard run.

Boundary values for all four dissolved nutrients as well as the validation data, including chlorophyll, were derived in the form of monthly mean values by Radach et al. (1996) and Radach and Pätsch (1997). For the two zooplankton groups of omnivorous mesozooplankton and carnivorous mesozooplankton, monthly mean values could be used from Broekhuizen and McKenzie (1995) based on continuous plankton recorder data. The trophic web in the COCOA system is closed by prescribing the grazing on zooplankton as well as the excretion of dissolved nutrients by fish and the flux from fish to the detritus pool.

3. Model results

3.1. Nutrient and chlorophyll concentrations

The distributions of nutrients and chlorophyll are shown for boxes lined up perpendicular to the coast, therefore representing different characteristics of the coastal region. The selected boxes 91, 82 and 64 are outlined in Fig. 1a. Box 91, the box where the Rhine

and the Meuse enter, exhibits high N/P ratios of up to 70 in the simulations. In box 82, a box off the coast but still in a region where gradients occur, the N/P ratios are between 16 and 35, providing a weak N-surplus. In contrast, box 64, in the central North Sea south of the Doggerbank, is characterised by simulated N/P ratios between 9 and 16 in 1988 and 15 to 17 in 1989.

The observed seasonal cycles of phosphate (Fig. 4a) and silicate (Fig. 4b) are simulated well for all three boxes. For nitrate (Fig. 4c) the river loads lead to higher values in box 91, while for boxes 82 and 64 the winter values of the simulations are too high. The rather poor simulation of the nitrate concentration especially in the winter period originates in the lack of knowledge about nitrification in the water column. Already during the first phase of the ERSEM project this problem was flagged (Radach and Lenhart, 1995) and despite different attempts to improve the model, a good agreement between model and observations could not be obtained for the whole range of nitrate concentration as observed in the North Sea. By using much smaller boxes in the COCOA setup than the previous setup ND15, a larger concentration range occurs and this problem is even more pronounced.

The simulation of chlorophyll (Fig. 4d) for box 91 is well within the range given by the measurements, while in the other two boxes the simulation exceeds the values of the measured chlorophyll concentrations in summer. However, the net primary production of 361 g C m^{-2} a^{-1} for box 91, 321 g C m^{-2} a^{-1} for box 82 and 224 g C m^{-2} a^{-1} for box 64 corresponds well with the measurements presented by Joint and Pomroy (1993) and Howarth et al. (1994) for the NERC North Sea Programme. Primary production is clearly decreasing with distance from the coast. In accordance with these values, the chlorophyll concentrations in Fig. 4d also decrease with distance from the coast. This is also true for the winter concentration of the nutrients, while the summer concentrations are reduced considerably due to the biological activity, as can be seen in Fig. 4a–c.

3.2. Integrated net primary production

To be able to compare the results of the COCOA setup with measurements and with results of other models, the COCOA results were mapped on the boxes of the setup ND15 (Fig. 1c). In Table 1 the simulated net primary production for 1988 and 1989 are given together with measurements by Joint and Pomroy (1993) and Van Beusekom and Diel-Christiansen (1994) as well as with output from the models ECOHAM (Moll, 1995, 1997) and NORWECOM (Skogen et al., 1995). Both models have a low trophic complexity, but a high spatial and temporal resolution compared to COCOA. In addition, for both models simulation results aggregated onto the ICES boxes are available from the literature, which allows a comparison with COCOA results mapped onto the setup ND15 of ERSEM. The ECOHAM is a three-dimensional primary production model simulating the phytoplankton–phosphate dynamics, which is driven by the same output from a three-dimensional baroclinic circulation model (Pohlmann, 1996a,b) and actual light forcing (Pätsch, 1994) as COCOA is. The NORWECOM is a coupled hydrodynamical–biological model, based on the general circulation Princeton Ocean Model, and the chemical–biological model part with seven state variables (four nutrients, two phytoplankton groups and detritus).

For the northern North Sea (boxes 1/11 and 2/12) the aggregated COCOA values for both years are slightly lower than values given by Van Beusekom and Diel-Christiansen (1994). The same is true for the values from ECOHAM, which correspond well with the COCOA values. Only the primary production simulated by the NORWECOM for box 1 exceeds the values from the literature. While there are no literature values available for the Norwegian Trench (box 3/13) the values of COCOA agree well with both models. The COCOA values for the central North Sea (boxes 4/14 and 5/15) for both years exceed both the literature values and the values from both three-dimensional models. For the Scottish coast (box 6) the low values for both years are a result of a limitation within the box model, since the box has a depth of 66 m and is not stratified in the setup ND15. The primary production values for both years from the COCOA simulation are close to the literature value of Van Beusekom and Diel-Christiansen (1994). In contrast, both three-dimensional models exceed this value nearly by a factor of 2.

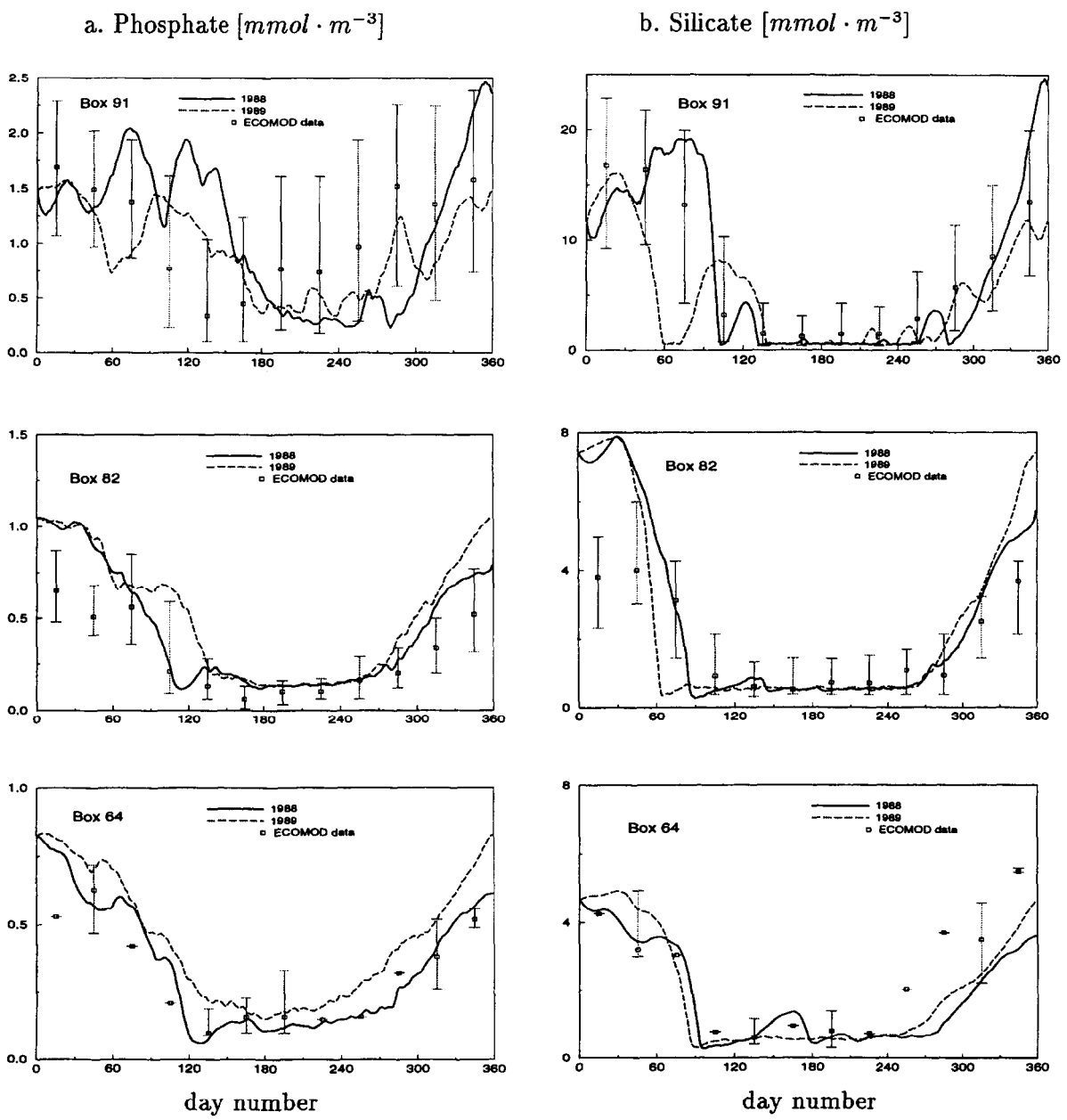

Fig. 4. Simulated concentration of (a) phosphate, (b) silicate, (c) nitrate, all in mmol m^{-3}, and (d) chlorophyll in mg Chl-*a* m^{-3} for the boxes 91, 82 and 64 for the years 1988 (thin line) and 1989 (dashed line) compared to monthly mean values derived from measurements (ECOMOD). The measurements from Radach et al. (1996) and Radach and Pätsch (1997) are presented in form of a median value (square) and ranges defined by the 17%- and the 83%-quantiles.

The aggregated COCOA values of annual net primary production for the English coast (box 7) are lower than the ones of Joint and Pomroy (1993) and Van Beusekom and Diel-Christiansen (1994). Both three-dimensional models give higher values, the NORWECOM being closest to the measurements but still a factor of 2 higher, while the ECOHAM gives slightly higher values than the COCOA results

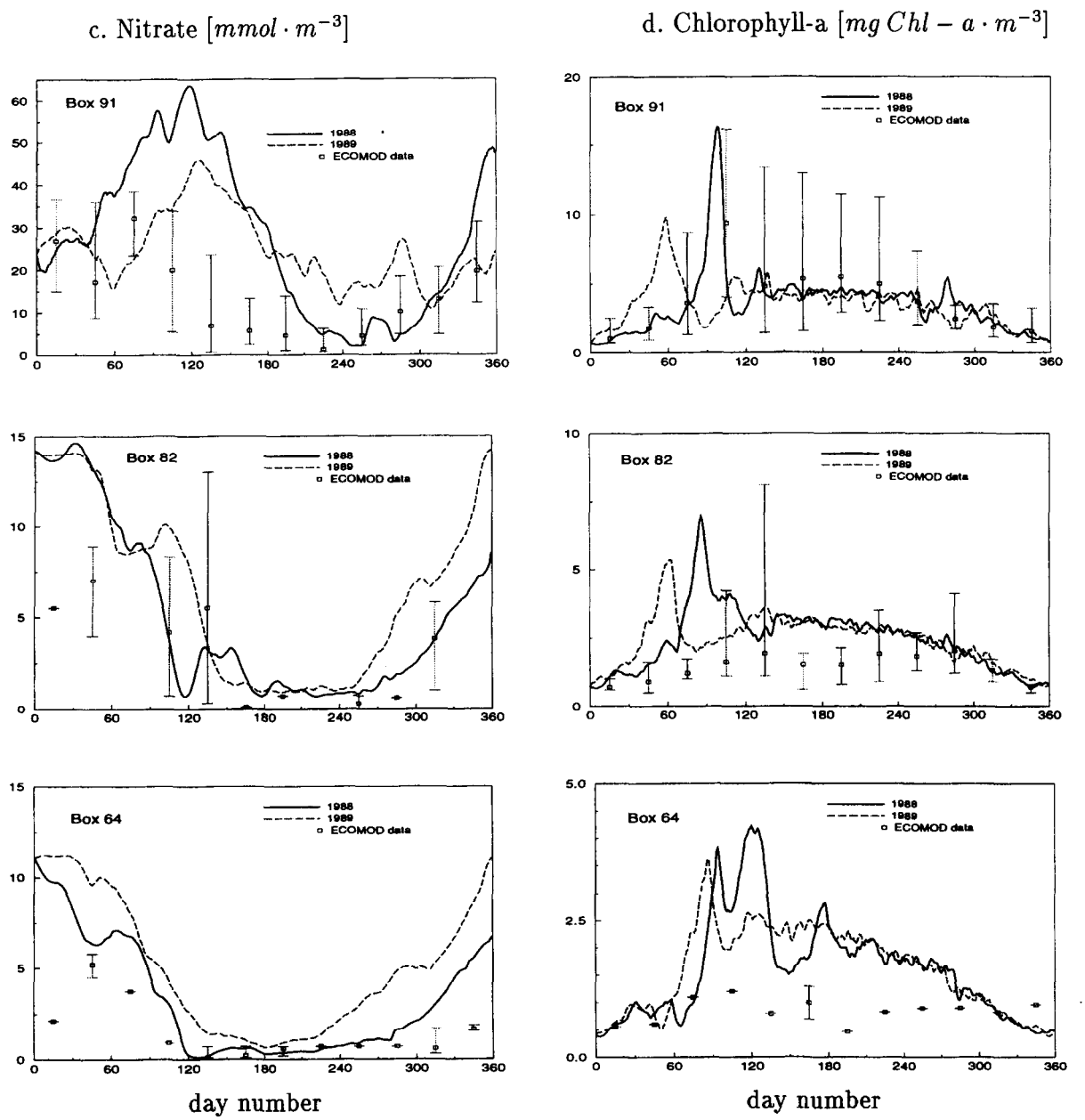

Fig. 4 (continued).

for 1989. We may conclude that the inclusion of suspended matter as forcing within COCOA is not strong enough to account for the effect the erosion of the English coast north of the Humber has on the attenuation and therefore on the primary production. For the Dutch coast (box 8), the COCOA values are higher than both literature values, but they are still near the high value given by Van Beusekom and Diel-Christiansen (1994). The model results by ECOHAM give a slightly lower value than the one aggregated from COCOA, while NORWECOM gives a much lower value. For the German Bight (box 9), the COCOA results are in good agreement with both literature values. For both three-dimen-

Table 1
Annual net primary production for the North Sea in g C m^{-2} a^{-1} from observations and models

Boxes		Observations		Model results			
ND15 box no.	ICES box no.	J & P 1988–1989	B & D 1980s–1990s	NORWECOM (3D model, 1985)	ECOHAM (3D model, 1986)	COCOA (aggregated, 1988)	COCOA (aggregated, 1989)
1+11	1	–	125	142	98	95	106
1+12	2	–	125	–	106	103	107
1+13	6	–	–	135	111	115	111
1+14	7A	100	–	99	119	135	137
1+15	7B	119	147	102	161	185	195
6	3A	–	75	141	138	57	60
7	3B	79	40	123	199	169	196
8	4	199	221	161	231	251	265
9	5A	261	240	128	233	247	264
10	5B	–	–	(128)	167	171	144

The results of COCOA are aggregated onto ND15.
J & P: Joint and Pomroy (1993); B & D: Van Beusekom and Diel-Christiansen (1994) and models.

sional models, the situation is the same as in box 8, with ECOHAM being close to the COCOA values, and NORWECOM giving an extremely low value. This mismatch in the coastal region is explained by Skogen et al. (1995) by a missing benthic remineralisation in the model. The comparison between the aggregated COCOA results and literature shows a good agreement of the COCOA simulation with observations, especially in the coastal region. For the northerly boxes, the correspondence is either also good, or shows the same deviation from the literature as the two three-dimensional models, e.g. for box 7.

Both for the southern and the northern North Sea in 1989 higher primary production can be observed than in 1988 in the COCOA results. For the southern North Sea, Klein and Van Buuren (1992) raised the question of how this could be, since river nutrient input was considerably higher in 1988 than in 1989. A possible explanation from the ERSEM forcing is, that in 1989 the solar radiation was more intense than in 1988. For the Dutch coastal area, the mean daily value was 114.3 W m^{-2} d^{-1} in 1989, compared to 104.5 W m^{-2} d^{-1} in 1988. The 1988 value is below and the 1989 value above the long-term mean value for the years 1955 to 1993 of 109 W m^{-2} d^{-1} given by Pätsch (1997). He also found a significant correlation between annual mean light intensity and annual net primary production for the southern North Sea.

3.3. Horizontal distribution of primary production and phosphate

In Fig. 5a the horizontal distribution of the net primary production is presented as simulated by COCOA for 1988. Values higher than 250 g C m^{-2} a^{-1} occur along the continental coast, with extreme values exceeding 300 g C m^{-2} a^{-1} at the Dutch coast, which correspond well with the findings by Peeters and Peperzak (1990). This is also in good correspondence with the distributions given by Joint and Pomroy (1993) for the southern North Sea, aggregated for 1988 and 1989 from measurements, as well as ECOHAM simulations by Moll (1997). Especially the contour representing 200 g C m^{-2} a^{-1} matches very well with the ECOHAM simulation. Joint and Pomroy (1993) found values grater than 300 g C m^{-2} a^{-1} also in parts of the German Bight and in the coastal area of southern Denmark. For the latter region a peak of high primary production of about 250 g C m^{-2} a^{-1} can also be observed in the distribution as simulated by COCOA (Fig. 5a). The elevated level of annual primary production of more than 250 g C m^{-2} a^{-1} west of southern Denmark also develops in the long-term simulations with the ERSEM setup ND130 over the years 1984–1993 (Pätsch and Radach, 1997). While this feature at the Danish coast is missing in the paper by Moll (1997), the peak of increased primary production on the Doggerbank, which is reproduced well by ECOHAM can only be

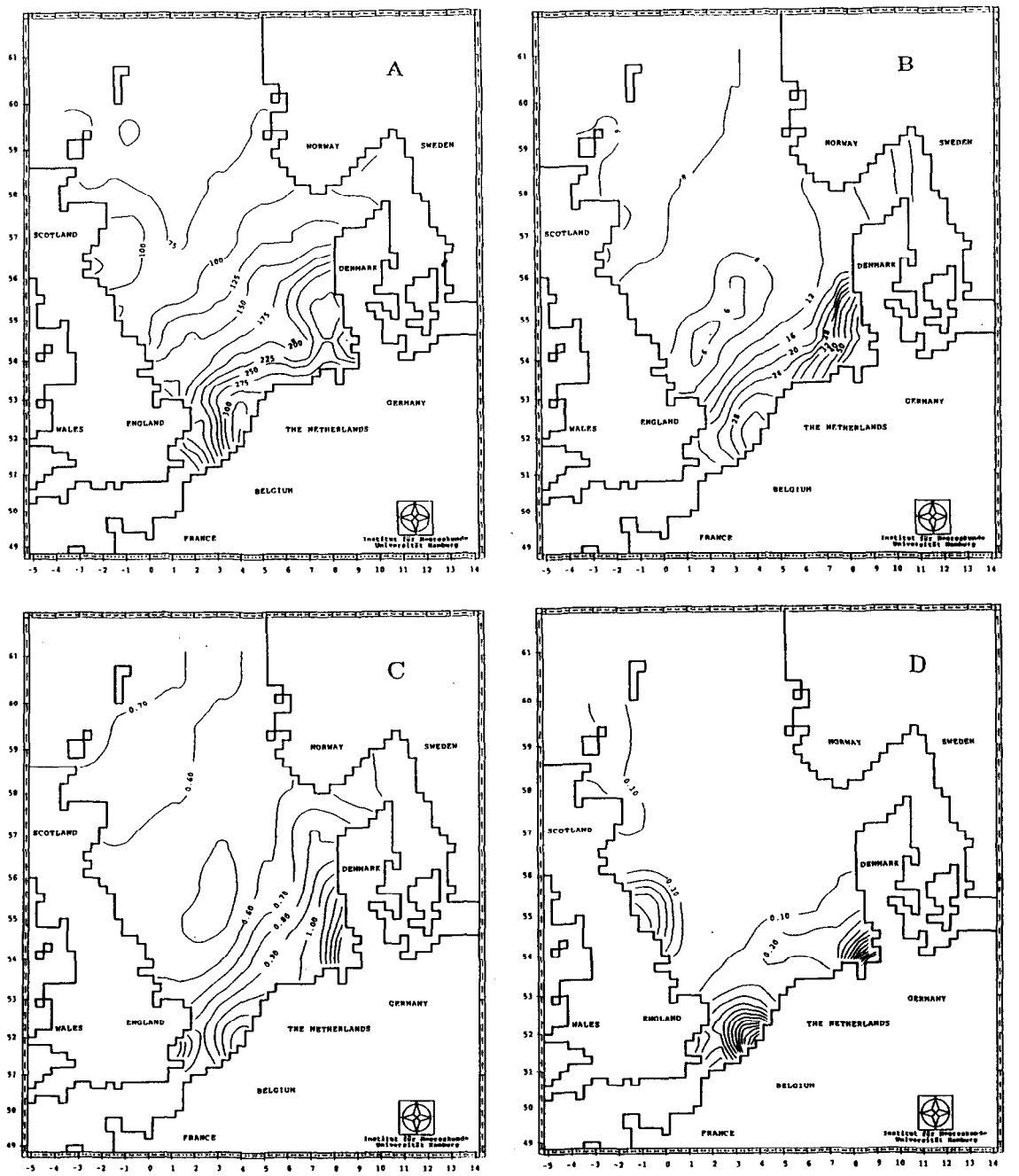

Fig. 5. Horizontal distributions simulated by COCOA for 1988 of (a) the net primary production in g C m^{-2} a^{-1}, (b) the monthly mean of the N/P ratio in the surface layer (0–30 m) for May and the phosphate concentrations for (c) February and (d) May in the surface layer (0–30 m) in mmol P m^{-3}.

seen in Fig. 5a as an extension of the 150 g C m^{-2} a^{-1} isopleth to the north in the COCOA simulation.

In Fig. 5b the N/P ratio is presented as simulated by COCOA for May 1988. Here the isopleth for the N/P ratio of 16 shows its widest extension to the north, representing the strongest spreading of

waters with a relative excess of nitrogen in the coastal area, which lasts from May till the end of July. The isopleth representing an N/P ratio of 16 matches quite well the isopleth for a primary production value of 200 g C m^{-2} a^{-1} (Fig. 5a), showing extended primary production in the coastal area with N/P ratios over 16 as a consequence of the river input. The influence of the continental rivers can be seen in areas with values over 30 along the Dutch coast and especially in the German Bight. We can conclude that the river input extends the area with an N/P ratio greater than 16 from the coast towards offshore regions, while low nutrient availability during summer still limits production.

The winter and summer distributions of phosphate are presented in Fig. 5c,d, representing the 1988 situation for February and May, respectively. In the winter phosphate distribution (Fig. 5c) large areas of the central and northern North Sea show concentrations of 0.6 to 0.7 mmol P m^{-3} whereas in summer (Fig. 5d) the concentration is reduced to 0.1 mmol P m^{-3}. In winter values greater 1.0 mmol P m^{-3} can be found in the continental coastal area and at the mouth of the Thames. While the summer concentration over the entire North Sea is much lower due to biological activity, the effect of the river inputs especially at the continental coast is very pronounced, as can be observed by the strong gradients.

3.4. Seasonal changes of mass flow nearshore and offshore

3.4.1. Nutrient limitations

Due to the river loads of the Rhine and the Meuse there is a high N/P ratio of up to 70 in box 91, with annual mean values of 30.5 for 1988 (Fig. 5b) and 34.8 in 1989. The load of all rivers entering box 91 leads to a simulated mean N/P ratio of 38.7, while the individual rivers show different ratios, e.g. 59.6 for the Meuse and 28.4 for the Rhine in 1988 and 69.1 and 35.8 for 1989, respectively. This high ratio indicates a relative excess of nitrogen in the box; but it does not indicate a P-limitation (Fig. 6a) in this box because of the generally high level of nutrients as discussed before. The only nutrient limitation in box 91 is of silicate (Fig. 6a), which occurs in one short single event in April and during a number of events between May and October. In box 82

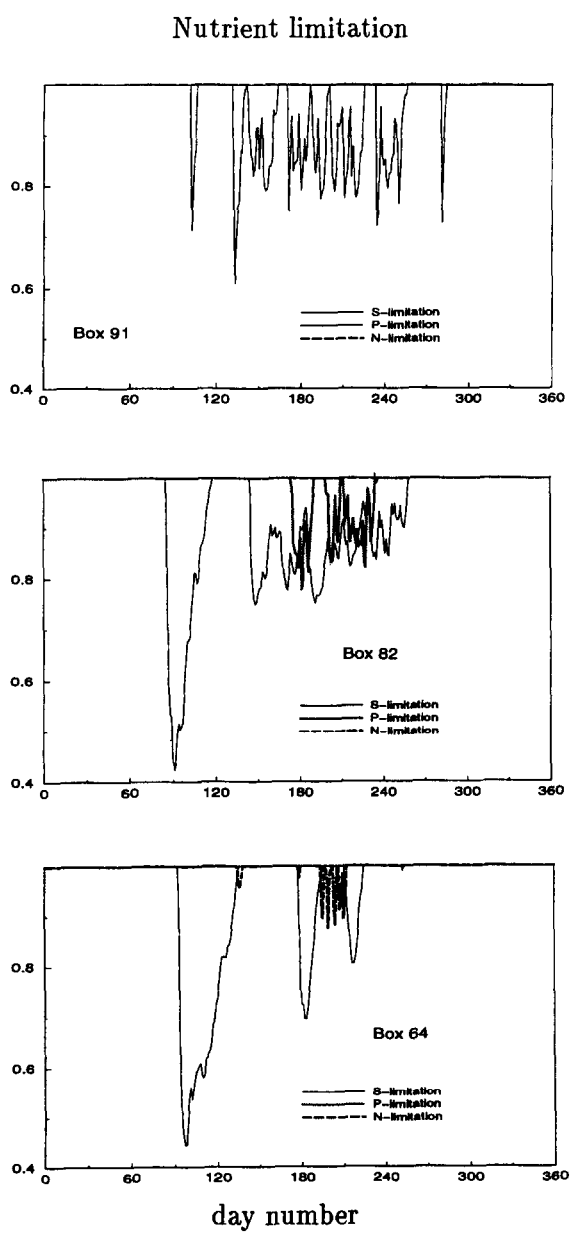

Fig. 6. Simulated limitation for silicon (thin line), phosphorus (dotted line) and nitrogen (dashed line) for diatoms for the boxes (a) 91, (b) 82 and (c) 64 for 1988. The value of the nutrient limitation function represents no limitation for the value 1 and increasing limitation for lower values.

(Fig. 6b) the first event is extended in time, and the limitation function reaches lower values indicating a stronger limitation. In summer, silicate limitation occurs during the same period as in box 91, but without

interruptions. Between July and September there is also a phosphate limitation. In box 64 (Fig. 6c) the first silicate limitation event is even more extended in time than in boxes 91 and 82, while during summer there are two short periods in July and August with silicate limitation. Between these periods a nitrogen limitation event can be observed, but no phosphate limitation. There is a shift from phosphate limitation to nitrogen limitation between boxes 82 and 64, which is in agreement with the N/P ratio. The effect of the river loads in box 82 is noticeable, both in the N/P ratio and in the occurrence of phosphate limitation. In contrast, in box 64 nearly central North Sea conditions are reached with an N/P ratio of less than 16 and nitrogen limitation, both for diatoms and picophytoplankton (not shown). In box 54 (not shown), north of box 64, the N/P ratio is about the same and all four phytoplankton groups in the model show nitrogen limitation.

3.4.2. Silicate dynamics

The time series for diatoms for the three selected boxes (Fig. 7a) differ in the magnitude of the biomass, showing lower concentrations with distance from the coast. The simulated zooplankton grazing of omnivorous mesozooplankton (Fig. 7b) represents about 90% of the total grazing on diatoms. One can clearly see a peak reaching up to 2.0 mmol Si m^{-3} d^{-1} in box 91 at the beginning of April. As there is no severe silicate limitation for the diatoms at this time (Fig. 6a), we conclude that in box 91 the diatom spring bloom is terminated by increasing grazing pressure. For boxes 82 and 64 the lower grazing pressure of e.g. 0.1 mmol Si m^{-3} d^{-1} for box 82, which is maintained throughout the summer, is insufficient by itself to terminate the bloom. In Fig. 7c the mortality flux from diatoms to detritus is shown as contribution to the detritus pool. Even in box 91, the total amount reaches at most 0.5 mmol Si m^{-3} d^{-1}, which is a factor of 4 less than the grazing seen in Fig. 7b at the same time. In contrast, the peaks of diatom mortality in boxes 82 and 64 are higher than the corresponding grazing fluxes. As there is a severe silicate limitation both in boxes 82 and 64 during the spring bloom peak, we conclude that the spring bloom of diatoms in both boxes was terminated by silicate limitation, leading to an increased flux of dead diatoms to detritus.

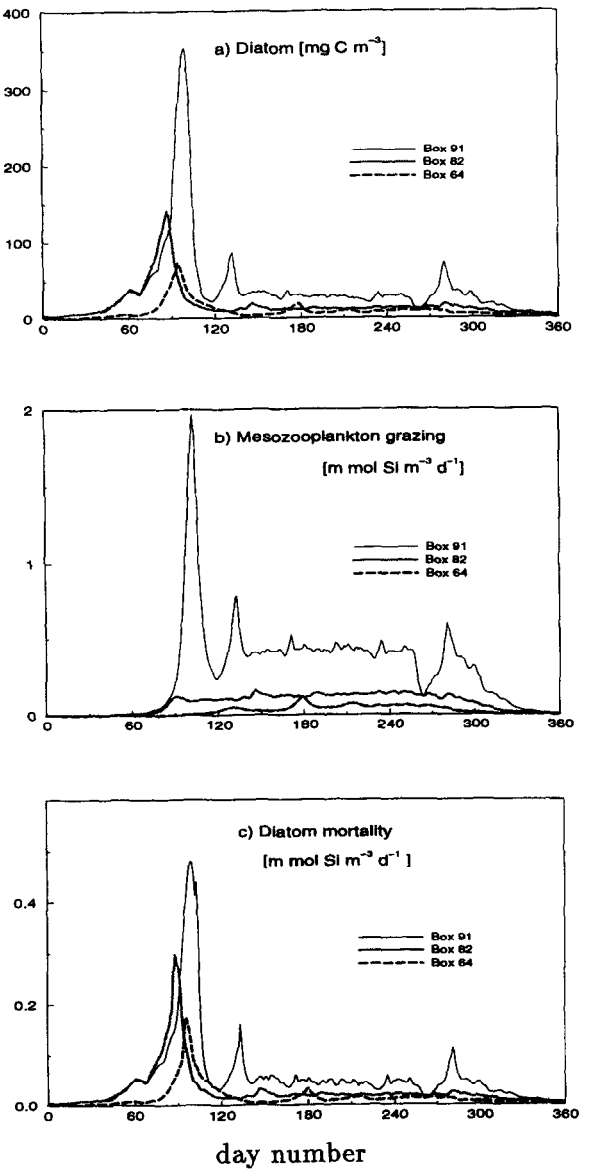

Fig. 7. Simulated concentration of (a) diatoms in mg C m^{-3}, the fluxes of (b) mesozooplankton grazing in mmol Si m^{-3} d^{-1} and (c) diatom mortality in mmol Si m^{-3} d^{-1} for the boxes 91 (thin line), 82 (dotted line) and 64 (dashed line) for 1988.

The major contributions to the dissolved silicate budget for box 91 are shown in Fig. 8a as annual cumulative fluxes in 10^6 kg for 1988 together with the silicate box content (bold line). In the first three months, the river input and the advective transport out of box 91 are the major processes. They are not

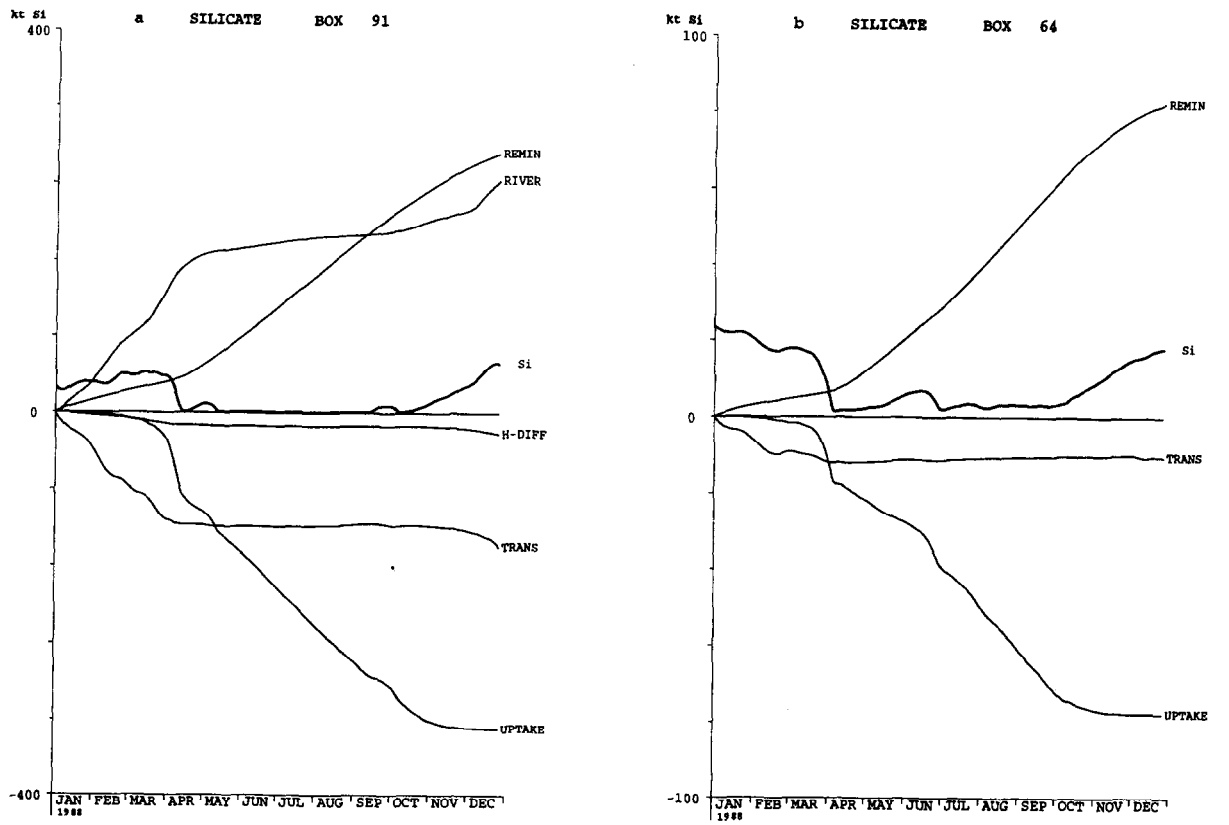

Fig. 8. Annual cumulative budget of silicate in 10^6 kg (kt) for the boxes (a) 91 and (b) 64 for 1988. The bold line represents the simulated silicate content of the box denoted as Si.

balanced, and the silicate box content is increasing. At the beginning of April, the uptake by diatoms increases which is mirrored after a time lag of about one month by remineralisation via the sediment. After the silicate pool has been drastically reduced due to uptake by diatoms at the beginning of April, the river input shows a reduced but nevertheless steady increase in its cumulative flux contribution to the silicate budget. In contrast there is no increase in the transport or in the horizontal diffusion until the dissolved Si-concentration begins to increase again. The provision of silicate by remineralisation and by the river input serves for uptake by the diatoms. This can be seen in a continuous increase of the cumulative uptake curve which agrees well with the fact that only episodic silicate limitations events occur in box 91. In the silicate budget for box 64 (Fig. 8b) the uptake of 78×10^6 kg and remineralisation of 82×10^6 kg are the major processes with only a small negative contribution by the transport of 11×10^6 kg. The beginning of the silicate limitation periods in April and June can be seen in the steps of the uptake curve.

The silicate budget for the diatoms in box 91 (Fig. 9a) clearly shows the cumulative grazing to be the strongest negative flux, and at the same time it mirrors the uptake flux as the strongest positive contribution in the budget. Therefore the conclusion that the diatom spring peak is stopped by grazing (Fig. 7b) can also be seen in the budget. Diatom mortality is always less than the grazing loss and shows only a small increase after a certain level is reached soon after the spring bloom. In contrast to the silicate budget for box 91 (Fig. 8a), only a small contribution by the transport to the diatom silicon budget occurs. In the corresponding budget for box 64 (Fig. 9b), the major difference is the high level of flux to the detritus relative to the grazing during the

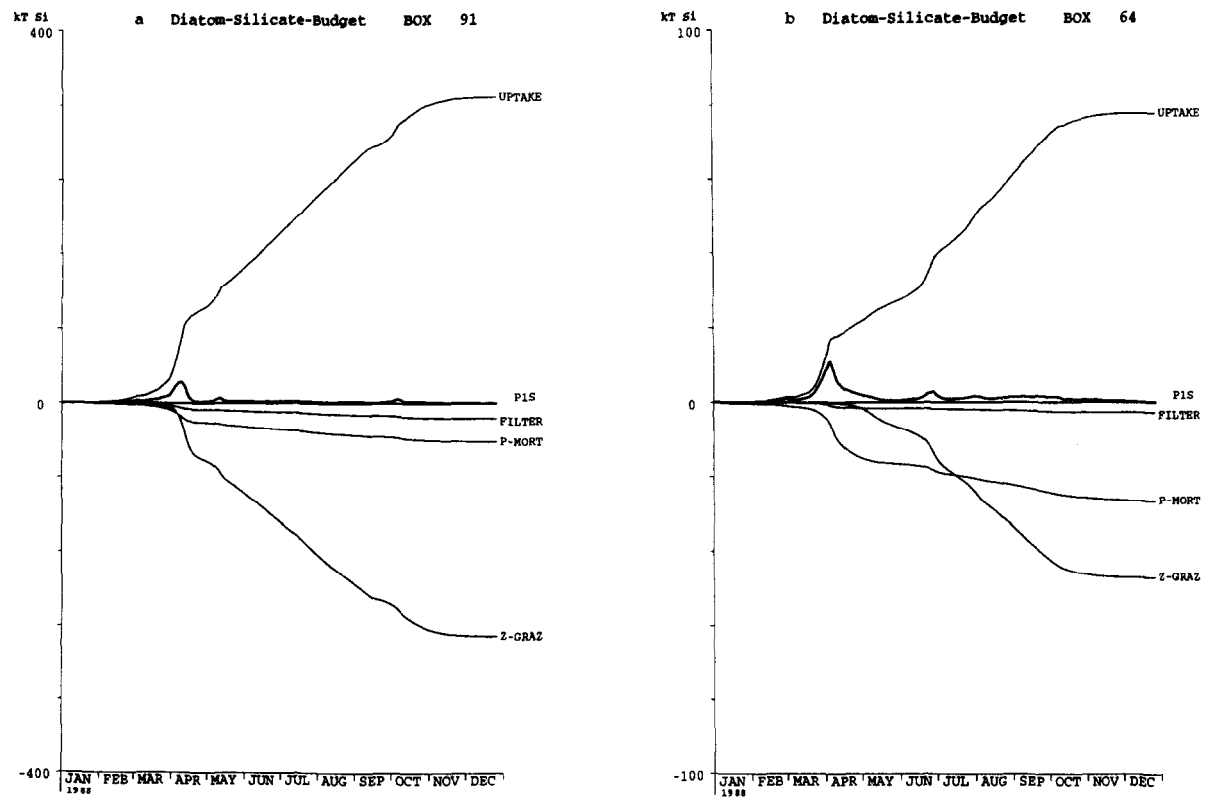

Fig. 9. Annual cumulative budget of diatom-silicate in 10^6 kg (kt) for the boxes (a) 91 and (b) 64 for 1988. The bold line represents the simulated diatom-silicate content of the box denoted as P1s.

period of the spring bloom. In addition, the detritus production exceeds the grazing from the beginning of February until the middle of July. Therefore, the spring bloom in box 64 was not governed by grazing, but was stopped by silicate limitation. At the same time diatom mortality has its strongest increase.

To quantify the effect of the different limitations acting within the ecosystem, we consider the resulting mass flows in the different boxes in relation to net uptake. In box 91, where zooplankton grazing was the major process balancing the nutrient uptake of silicate by diatoms, 76% of net uptake contributes to the zooplankton and 13% goes into detritus production. In box 82 the zooplankton receives 66% of the net uptake and in box 64 this is only 60%. Along with this reduction in the zooplankton grazing on diatoms goes an increase in the contributions to the detritus pool of 22% in box 82 and 35% of the net uptake in box 64.

3.4.3. Phosphorus and nitrogen

The internal dynamics of the different boxes, as discussed on the basis of the silicate budget in the previous chapter, is acting on the scale of the pelagic ecosystem as a whole. A standardised format for showing the budgets has been developed which allows direct comparisons between the boxes, e.g. Figs. 10 and 11. The squares indicate state variables or sum of state variables, while big arrows give the fluxes between the state variables, integrated over one year (in 10^6 kg), as there are nutrient uptake by phytoplankton (DIP→PHY), grazing of zooplankton on phytoplankton (PHY→ZOO), excretion of nutrients by zooplankton (ZOO→DIP), loss of zooplankton to detritus (ZOO→DET), grazing of zooplankton on bacteria (BAC→ZOO), feeding of bacteria on detritus (DET→BAC) and the uptake (DIP→BAC) or the excretion (DIP←BAC) of nutrients by bacteria depending on the direction of the arrow. In addition the inputs by the rivers and, for nitrogen also by the

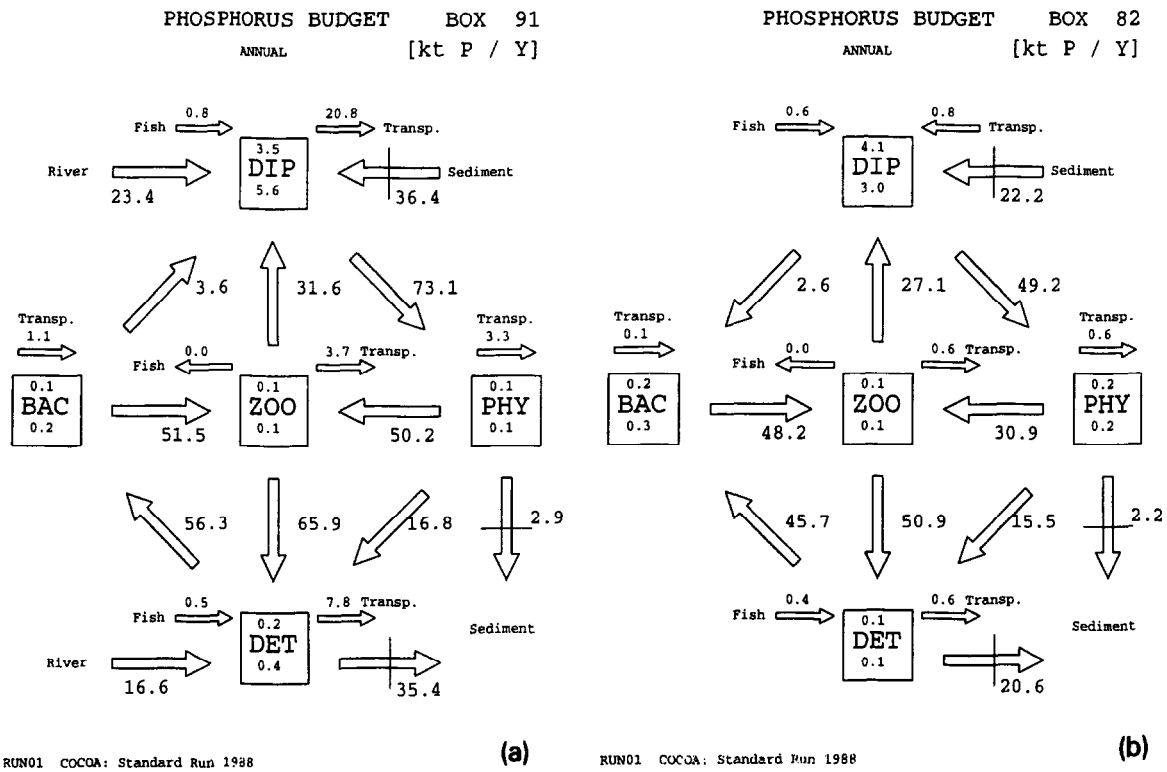

Fig. 10. Annual phosphorus budget for 1988 in 10^6 kg (kt) for box (a) 91 and (b) box 82. The squares indicate state variables or sums of state variables in the model, e.g. *DIP* for phosphate, *PHY* for the sum of all four phytoplankton groups, *ZOO* for the sum of the three zooplankton groups, *DET* represents detritus as sum of POM and DOM and *BAC* for bacteria. The number above the state variable shows the initial box content and the one below the content at the end of the simulation in 10^6 kg. The big arrows give the fluxes between the state variables, the river input, and the sedimentation, while the smaller arrows mark the contribution of advective and diffusive horizontal transport and fish.

atmosphere, are indicated as well as the fluxes from or to the sediment. For phytoplankton and detritus the flux into the sediment represents the sum of two different processes, one being the sinking of phytoplankton or detritus and the second the activity of the benthic filter feeders on these two pelagic state variables. The smaller arrows mark the contributions of advective and diffusive horizontal transport and the interaction with fish as next trophic level.

Of the 23.4×10^6 kg phosphorus river input to box 91 (Fig. 10a) 87% is directly transported away from the box. The uptake of phosphorus by the phytoplankton (73.1×10^6 kg) is the highest flux in the budget for box 91. Compared to phytoplankton uptake, an amount of 69% is grazed by zooplankton and 23% ends as contributions to detritus by mortality. The excretion losses by the zooplankton to the inorganic nutrient pool make up about 43% of the nutrient uptake. With this return flow to the inorganic nutrient pool a first cycle, here called the autotrophic loop, is closed. The zooplankton feeding on bacteria with 70% of the nutrient uptake yields an even higher input to the zooplankton than the grazing on phytoplankton. This high rate of grazing of zooplankton on bacteria is supported by a strong flux from zooplankton to detritus, which makes up 90% of the nutrient net uptake. The contributions to the detritus pool both by phytoplankton and zooplankton mortality allow a high amount of detritus material to be taken up by bacteria, i.e. about 77% of the net uptake. Therefore we can recognise an important second cycle representing the heterotrophic loop, starting with contributions to the detritus pool by zooplankton mortality, continuing with bacterial uptake and ending with zooplankton grazing on bacteria. In box 91 the heterotrophic loop is supported

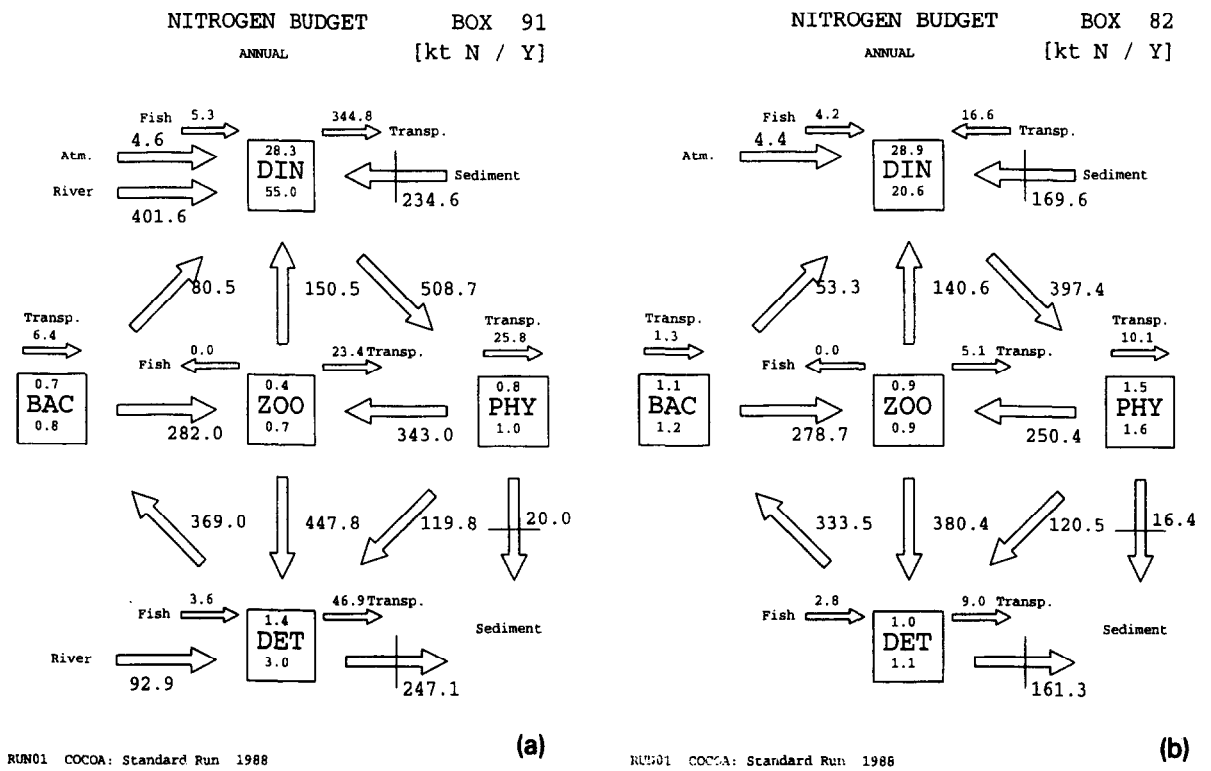

Fig. 11. Annual nitrogen budget for 1988 in 10^6 kg (kt) for (a) box 91 and (b) box 82. *DIN* represents the sum of nitrate plus ammonium. Above the river input the contribution by atmospheric nitrogen loads is indicated. See further the legend of Fig. 10.

by the additional input of organic material by the rivers into the detritus pool, which is about 70% of the river input to the inorganic nutrient pool. The total of phytoplankton and detritus losses to the sediment of 38.3×10^6 kg nearly balances the remineralisation flux from the sediment to the inorganic nutrient pool of 36.4×10^6 kg, leaving a small net gain for the sediment of 1.9×10^6 kg or 3% of the net nutrient uptake by the phytoplankton.

A comparison of the pelagic phosphorus budget for the offshore box 82 in 1988 (Fig. 10b) with the one for box 91 still shows the two major pathways as described for box 91, but they have changed their relative importance within the ecosystem in box 82. The missing input by the river in box 82 in combination with the lower winter concentration results in a reduced net uptake of nutrients by phytoplankton of 33% compared to box 91. Note that the higher volume in box 82 than in box 91 results in a higher amount of phosphorus in the box, even though the phosphorus concentration is lower, e.g. the winter concentration is 1.4 mmol P m^{-3} in box 91 compared to 1.0 mmol P m^{-3} in box 82. These reduced winter concentrations cause a silicate and phosphate limitation in box 82, as presented earlier. Of the 49.2×10^6 kg phytoplankton uptake about the same amount is grazed by zooplankton (63%) or lost to the sediment (4%) as in box 91. In contrast, the flux towards the detritus pool by phytoplankton mortality has increased to 32% compared to 23% in box 91. In box 82 the contribution to detritus by zooplankton mortality exceeds even the nutrient uptake, showing a shift in the relative importance towards the heterotrophic loop. Because of the missing inorganic river load leading to nutrient limitation, the recirculation of organic material via bacteria is the major mass flow in the ecosystem in box 82. The input to the sediment both by phytoplankton and zooplankton of 22.8×10^6 kg exceeds the remineralisation of 22.2×10^6 kg by 0.6×10^6 kg. In box 64 (not shown here) the net uptake is even more reduced to 53% of that in box 91. Generally the same shift to the heterotrophic loop as the dominant mass flows can be observed.

The phosphorus budgets of the individual phytoplankton groups (not shown here) reveal an increased detritus production off the coast especially for flagellates and dinoflagellates, despite a lower net uptake due to nutrient limitation at the same time. This results mainly in a lower zooplankton grazing on diatoms, flagellates and dinoflagellates. This corresponds with an increased grazing of zooplankton on bacteria, since the bacteria show a stronger feeding on the higher detritus pool.

There are some structural differences between the nitrogen budget (Fig. 11a) and the phosphorus budget (Fig. 10a) for box 91. The first is the additional input from the atmosphere of 4.6×10^6 kg, which is only about 1% if the inorganic input by the rivers. The second is an additional loss term for nitrogen in the sediment. This loss represents the process of denitrification in the sediment, by which 15.8×10^6 kg are removed from the system. In addition, the inorganic nutrient input from the river loads into the organic pool makes up a fraction of only 23%, while in the phosphorus budget the relation was 70%. In contrast, the amount of detritus lost to the sediment is higher in the nitrogen budget than in the phosphorus budget. Here, the input by detritus alone already exceeds the remineralisation to the inorganic nutrient pool by the sediment. The higher input of detritus to the sediment in box 91 results in a lower mass flow through the heterotrophic loop. Furthermore, the excretion by bacteria into the inorganic nutrient pool has increased to 16% of the net uptake in box 91, compared to 5% in the phosphorus budget. This is balanced by the zooplankton excretion which is reduced to 30% of the net uptake compared to 43% in the phosphorus budget. Therefore, we conclude that the nitrogen budget for box 91 shows a stronger dominance of the autotrophic loop than the phosphorus budget.

In the nitrogen budget for box 82 (Fig. 11b) the input by the atmosphere is the only external source of inorganic nutrients. This affects the nitrogen uptake by phytoplankton, which is 22% lower than in box 91, even though the net uptake remains the strongest flux. The heterotrophic loop is fed by a slightly higher grazing than in box 91 but loses considerably by bacterial excretion of about 13% of the net uptake in box 82, while there was a net gain to the bacteria in the phosphorus budget. Generally there is the same tendency to a relatively stronger heterotrophic loop in box 82 than in box 91 both in the nitrogen budget and in the phosphorus budget. But for box 82 the dominant mass flow in the nitrogen budget is still within the autotrophic loop. Only in box 64 (not shown here) has this tendency to a stronger heterotrophic loop offshore reached the same level as in the phosphorus cycle, with the flux from zooplankton to detritus exceeding the net uptake of nutrients by phytoplankton.

The nitrogen budget of the diatoms (not shown here) shows the grazing by omnivorous mesozooplankton on diatoms to reach about the same level as the net uptake of nitrate in all three boxes. However, in the coastal box 91 the start of this grazing by omnivorous mesozooplankton follows with a time shift nearly parallel to the nitrate uptake. Therefore, the spring bloom is ended by this increased grazing pressure in box 91. In contrast, in the offshore boxes 82 and 64 the zooplankton grazing by omnivorous mesozooplankton follows the ammonium uptake. Only after the spring bloom do the ammonium and the omnivorous mesozooplankton grazing start to increase and reach the same level as the nitrate uptake in boxes 64 and 82. Therefore, nutrient limitation terminates the spring bloom in boxes 82 and 64, leading to increased mortality and contributions to the detritus pool, while the zooplankton grazing follows the production fed by ammonium regeneration. This results in considerable differences in the uptake of nitrate and ammonium by diatoms and flagellates. While the uptake in box 91 is 108×10^6 kg nitrate and 30×10^6 kg ammonium for diatoms and 101×10^6 kg nitrate and 37×10^6 kg ammonium for flagellates these values change towards an increased uptake of ammonium in the offshore boxes. The corresponding values for box 82 are 33×10^6 kg nitrate and 29×10^6 kg ammonium for diatoms and for flagellates 58×10^6 kg nitrate and 87×10^6 kg ammonium. Thus the ammonium uptake by flagellates exceeds the one of nitrate uptake in box 82. The same goes for box 64.

4. Reduction scenarios

Scenarios were run to test the effect of reduction of the riverine nutrient load, the effect of neglecting the particulate organic matter load and of the atmospheric input in the forcing of the model. All sce-

nario model runs were carried out in the same way as the standard runs by running a simulation with the scenario setup over 30 years to obtain repeating annual cycles. The simulation results represent the ecosystem model in a new steady state which has adapted itself to the new forcing.

For the river loads three different scenario runs were carried out, applying a 25% reduction in scenario A, a 50% reduction in scenario B and a 75% reduction of the river loads in scenario C. In these scenarios the phosphorus and nitrogen input was reduced as inorganic and organic load, but there is no reduction of inorganic silicate since there is no evidence for a reduction of inorganic silicate over the years in the literature (Van Bennekom et al., 1975). For the particulate organic matter, however, the silicate is reduced in the same way as the other organic compounds.

4.1. Effects on the primary production

In Table 2 the annual net primary production values are presented for the five different scenarios for both years, aggregated into the 15 boxes of the setup ND15 (Fig. 1c). As expected, the highest effects of the reduced river loads are found in boxes 8 and 9, representing the continental coastal zone, and the English coastal box 7. These boxes show a reduction of net primary production of more than 6% in scenario A, about 14 to 15% in scenario B and between 21 and 30% in scenario C in comparison with the standard run. In 1988, the highest effect was in the Dutch coastal box 8 with 17% difference in scenario B and 30% in scenario C. In 1989 the highest values of 16% in scenario B and 30% for scenario C were in the German Bight box 9. This is also the highest effect found in all boxes for the river scenarios.

There is almost no effect on the aggregated net primary production of the reduced river load in the northerly boxes 1/11 and 2/12. Also, little effect of the different river scenarios is found in the Scottish coastal box 6. This is surprising, since there are sources of river input acting in this box, e.g. the Firth of Forth, but they are rather small compared to the

Table 2
Comparison of annual net primary production from five different scenarios for the North Sea in g C m^{-2} a^{-1} for 1988 and 1989

ND15 box no.	Standard run	COCOA scenarios				
		A (25% red.)	B (50% red.)	C (75% red.)	D (no atm.)	E (no POM)
COCOA 1988						
1+11	95	94 (1.1)	93 (2.2)	91 (4.3)	90 (5.3)	93 (2.2)
2+12	103	102 (1.0)	101 (2.0)	99 (3.9)	95 (7.8)	101 (2.0)
3+13	115	109 (5.3)	107 (7.0)	106 (7.9)	102 (11.4)	109 (5.3)
4+14	135	130 (3.7)	129 (4.5)	127 (6.0)	116 (14.1)	131 (3.0)
5+15	185	174 (6.0)	165 (10.9)	155 (16.3)	159 (14.1)	178 (3.8)
6	57	56 (1.8)	56 (1.8)	56 (1.8)	52 (8.8)	56 (1.8)
7	169	158 (6.5)	146 (13.6)	133 (21.3)	148 (12.4)	163 (3.6)
8	251	233 (7.2)	209 (16.7)	176 (29.9)	241 (4.0)	231 (8.0)
9	247	232 (6.1)	210 (15.0)	176 (28.7)	242 (3.0)	225 (9.0)
10	171	158 (7.7)	147 (14.0)	135 (21.1)	156 (8.2)	162 (6.0)
COCOA 1989						
1+11	106	105 (1.0)	101 (4.7)	99 (6.6)	99 (6.6)	101 (4.8)
2+12	107	106 (1.0)	102 (4.7)	100 (6.6)	98 (8.5)	101 (5.7)
3+13	111	108 (2.8)	106 (4.6)	101 (9.0)	100 (10.0)	103 (7.3)
4+14	137	134 (2.2)	131 (4.4)	127 (7.3)	117 (14.6)	130 (5.2)
5+15	195	180 (7.7)	174 (10.8)	167 (14.4)	167 (14.4)	185 (5.2)
6	60	59 (1.7)	59 (1.7)	58 (3.4)	55 (8.4)	59 (1.7)
7	196	183 (6.7)	169 (13.8)	155 (21.0)	172 (12.3)	189 (3.7)
8	265	249 (6.0)	229 (13.6)	201 (24.2)	253 (4.6)	247 (6.8)
9	264	245 (7.2)	219 (16.1)	185 (30.0)	253 (4.2)	239 (9.8)
10	144	131 (9.0)	126 (12.5)	122 (15.3)	126 (12.5)	133 (7.7)

The numbers in brackets denote the reduction in percent compared to the standard runs.

river nutrient loads by the Rhine or the Meuse. The Norwegian Trench (box 3/13) shows consistently larger effects than the central North Sea (box 4/14), probably as a result of the outflowing water masses from the continental coastal region via the Norwegian Trench, while box 4/14 is still governed by the short recirculation system of Atlantic inflow water. In box 5/15 the effects of the reduced river loads can clearly be seen in a difference of the net primary production of up to 8% in scenario A, 11% in scenario B and 16% in scenario C compared to the standard run. Here the effect on the neighbouring coastal boxes can be observed to the same degree as in the Danish coastal box 10, through which passes the outflowing water of the continental coastal region. Overall the influence of reduced river loads is strongest in the continental coastal boxes and to a lesser degree in the northerly box 5/15 or the outflow boxes 10 and 3/13. This is in agreement with Klein and Van Buuren (1992), who argued that the discharges from the major rivers hardly affect the central North Sea as a result of the prevailing current patterns.

Two additional scenarios were run with the atmospheric input (scenario D) or the river load of particulate organic matter (scenario E) set to zero. For scenario D, where the atmospheric nitrogen input is neglected, the net primary production is reduced between 3% and 14% compared to the standard runs. The highest effect with up to 15% can be found in boxes 4/14 and 5/15 for both years, followed by box 7 with 12% and 11% for box 3/13. The continental coastal boxes 8 and 9 show a much lower effect of less than 5% of the annual primary production in comparison with the standard runs for both years. The effect of neglecting atmospheric nitrogen input can be compared to the effect of the reduction of the river loads for boxes of the central North Sea, but it does not have a big influence on the continental coastal boxes where the effect of the river input is strongest.

In scenario E, where the particulate organic matter loads are neglected, the highest differences can again be found in the continental coastal boxes 8 and 9 with up to 10% difference to the net primary production of the standard run. The outflowing boxes 10 and 3/13 both give values of about 7%, while the English coastal box 7 with about 4% shows a reduced response to this kind of forcing. This shows that neglecting the particulate organic river load has a major effect on the same boxes as the reduction of the inorganic river loads. Overall the difference in the annual net primary production compared to the standard run can reach 10%. This is, however, lower than the effect of neglecting the atmospheric nitrogen load.

4.2. Effects of a 50% reduction of the river loads on the ecosystem

The effects of scenario B, a 50% reduction of the river loads, will be presented here in more detail. When comparing the simulated phosphate concentrations for the standard run to scenario B for boxes 91 and 82 (Fig. 12a,b), we can clearly see the reduced level of phosphate concentration in winter but also in summer in both boxes. As expected, the differences are lower in the offshore box 82. The same

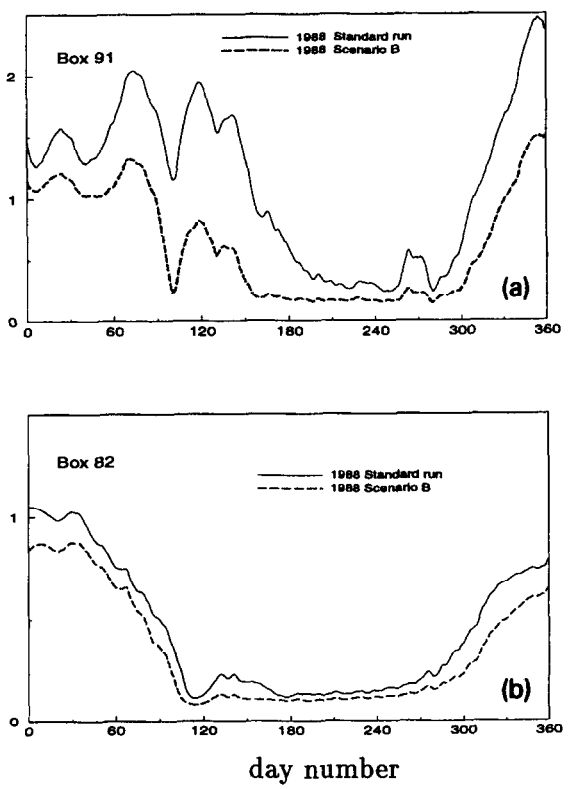

Fig. 12. The simulated phosphate concentrations for boxes 91 (a) and 82 (b) as standard run (thin line) and the scenario B run (dashed line), with a 50% reduction in river load for 1988 in mmol P m^{-3}.

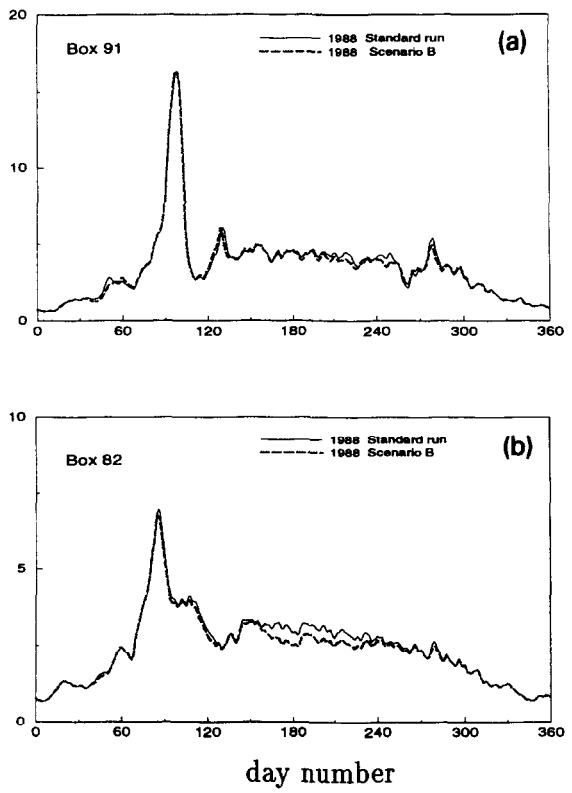

Fig. 13. The simulated chlorophyll-*a* concentrations for boxes 91 (a) and 82 (b) as standard run (thin line) and the scenario B run (dashed line), with a 50% reduction in river load for 1988 in mg Chl-*a* m^{-3}.

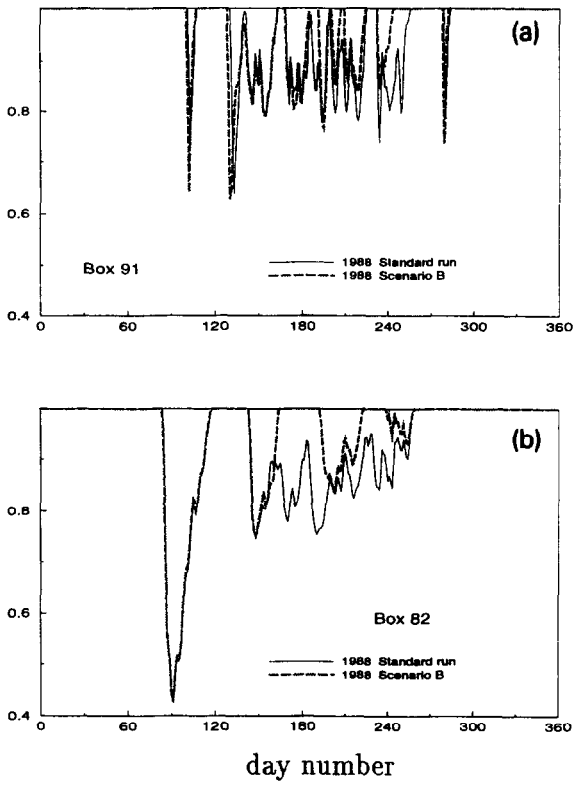

Fig. 14. The simulated silicate limitation functions for boxes 91 (a) and 82 (b) as standard run (thin line) and the scenario B run (dashed line), with a 50% reduction in river load for 1988.

can be seen for the other nutrients (not shown here), with the lowest effect on the silicate concentration. In contrast, looking at the corresponding chlorophyll time series (Fig. 13a,b), shows that the difference between the two runs is very small. Both boxes show about the same level in the spring peak, while the standing stocks over the summer exhibit differences, especially in box 82 (Fig. 13b).

This can partly be explained from the nutrient limitations in both boxes, e.g. for the diatoms. In the silicate limitation function in box 91 (Fig. 14a) a series of short-term events occur. In box 82 (Fig. 14b) the silicate limitation functions are nearly the same in both runs during the spring peak and in early summer. However, the long period of silicate limitation during summer in the standard run is broken up into three smaller periods with no limitations acting in between in the scenario run. When comparing the phosphate limitation function acting in box 91 (Fig. 15a), phosphate limitation occurs in summer in the reduction run while there is no limitation in the standard run. In box 82 (Fig. 15b) the small phosphate limitation in summer in the standard run is extended in intensity and in time in the scenario B run. For the nitrogen limitation (not shown here) a short period of limitation occurs in box 91; a more intensive limitation occurs in box 82, while there was no limitation in the standard run. In conclusion, because there are no differences in the silicate limitation during the spring bloom there are no differences at this time in the chlorophyll time series. As phosphate and nitrogen limitations begin to act in the reduction run during summer, obvious differences in the corresponding chlorophyll concentrations develop. Moreover, as the other limitations are still acting, the silicate limitation is weaker especially during the end of the summer.

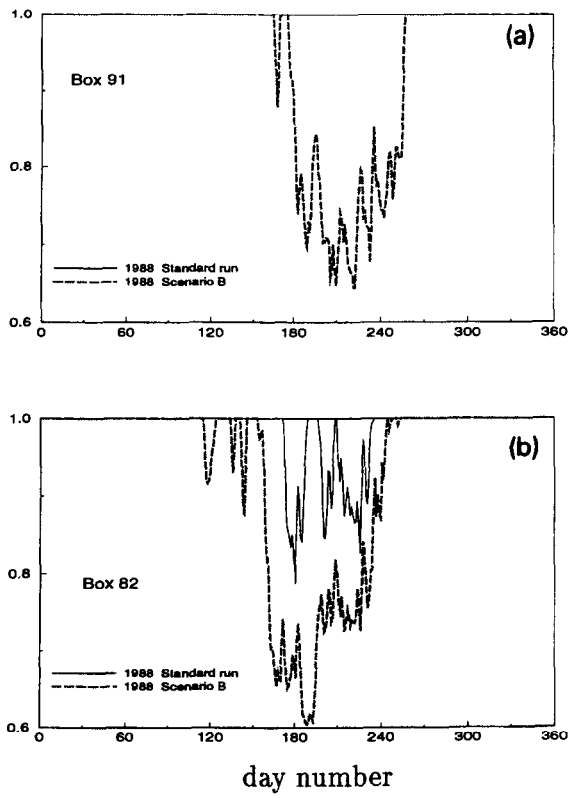

Fig. 15. The simulated phosphate limitation functions for boxes 91 (a) and 82 (b) as standard run (thin line) and the scenario B run (dashed line), with a 50% reduction in river load for 1988.

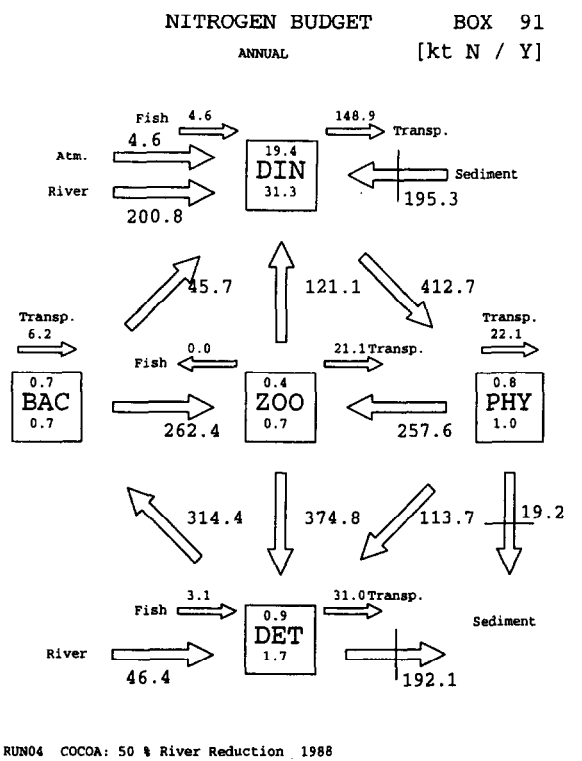

Fig. 16. Annual nitrogen budget for the scenario B run, with a 50% river reduction in 1988, in 10^6 kg (kt) for box 91. See further the legends of Figs. 10 and 11.

Finally, in the nitrogen budget for the pelagic ecosystem in box 91 (Fig. 16) for the 50% river reduction scenario B, the net uptake constitutes 81% compared to the nitrogen uptake in the standard run (Fig. 11a). The difference of 19% is more than the corresponding difference of the net primary production for box 8 in Table 2. In box 82 (not shown here) the difference in the nitrogen uptake amounts to 37% of the uptake in the standard run. While the nitrogen uptake in box 91 is reduced in the reduction scenario run, the loss terms of phytoplankton make up 28% due to mortality. The zooplankton grazing on phytoplankton is lower than in the standard run, but the heterotrophic loop shows a higher amount of net uptake than the standard run. Even though the overall uptake is reduced in the scenario run, the ammonium uptake by diatoms and flagellates has increased, while the nitrate uptake has decreased, indicating a drastic change in the uptake relations. In contrast, the comparison of the annual net primary production gives only a small hint of the changes occurring in the dynamics of the reduction scenarios, while major differences in uptake or further mass flows through the ecosystem yield quite similar primary production values.

5. Discussion and conclusion

To describe the ecosystem dynamics in the continental coastal zone, the ecosystem model ERSEM was used in the frame of the COCOA setup by reducing the size of the boxes especially in the coastal areas. The realistic forcing, which was adopted for this setup, provided answers to the question raised by Klein and Van Buuren (1992), why there was a higher net primary production in the southern North Sea in 1989 than in 1988, even though the nutrient river loads in 1989 were lower. The reason appears to be a higher solar energy input in 1989 by about 10 W

m^{-2} d^{-1}, than in 1988. This increase of solar energy overcomes the effects of a smaller river nutrient load by providing more light for primary production.

Comparison of simulated nutrient concentrations with measurements showed a good agreement for nutrients which exhibit a clear seasonal cycle. However, for some boxes the simulated winter concentrations of the nutrient tended to be higher than observed. While the simulated chlorophyll concentrations showed higher values in the onshore boxes, the annual net primary production decreased away from the coast which is in good agreement with data (Joint and Pomroy, 1993). The comparison between the aggregated COCOA results and numbers given by Joint and Pomroy (1993) and Van Beusekom and Diel-Christiansen (1994) shows a good agreement of the COCOA simulation especially in the coastal region. For the northern boxes, the accordance is also good or shows the same deviation from the literature as the two three-dimensional models ECOHAM (Moll, 1995, 1997) and NORWECOM (Skogen et al., 1995). Furthermore, strong horizontal gradients as simulated by COCOA could be presented in the horizontal distributions of the net primary production and the phosphate concentration. The extension of the influence by the river loads on the ecosystem could also be demonstrated by the distribution of the isopleth representing an N/P ratio of 16.

Based on the N/P ratios, three different boxes were selected to represent different dynamics of the coastal ecosystem. A high N/P ratio indicating a nitrogen surplus in the box where Rhine and Meuse enter does not necessarily mean a phosphate limitation, because of the high levels of nutrients introduced by the rivers. In fact, there is only a small silicate limitation in this coastal box, while the causes of the limitation change towards offshore regions from a phosphate limitation to a nitrogen limitation near to the central North Sea, always in addition to a strong silicate limitation in these offshore boxes. Because there is no severe silicate limitation in the coastal box, the diatom spring bloom is stopped by increased grazing pressure, while in the offshore boxes the spring bloom was ended by silicate limitation, leading to an increased flux to detritus due to increased diatom mortality. Therefore the major difference between the coastal box and the offshore boxes is the increase of the flux to detritus relative to the grazing during the period of the spring bloom. To show the effect on the ecosystem as a whole, the resulting mass flows in the different boxes in relation to the net uptake were quantified to be a loss of about 16% for the zooplankton grazing on diatoms and a gain of 20% for the flux to the detritus in relation to the net uptake towards offshore regions.

Furthermore, two different cycles of mass flow for phosphorus and nitrogen were identified. The first, denoted as the autotrophic loop, starts with the net uptake as the strongest flux occurring in the coastal box. The importance of the second cycle, representing the heterotrophic loop, can also be shown in the coastal box, because in this box the zooplankton feeding on bacteria is higher than the zooplankton grazing on phytoplankton. In the coastal box the heterotrophic loop is supported by the additional input of organic material from the rivers, which is about 70% of the river input of phosphate to the inorganic nutrient pool. In the offshore box the missing input by the river in combination with the lower winter concentration results in a reduced net uptake of phosphate by phytoplankton of 33%, compared to the coastal box. There is a general shift in the relative importance of the cycling towards the heterotrophic loop. The contributions by zooplankton mortality to detritus exceeded the nutrient uptake towards offshore regions. The missing inorganic river load leads to nutrient limitation, and detritus production increases towards offshore regions, especially by flagellates and dinoflagellates, leaving the mineralisation of organic material by bacteria as the major nutrient mass flow in the ecosystem.

In the nitrogen budget, the additional atmospheric input corresponds only to about 1% of the river contributions in the coastal box. Compared to the input to the inorganic nutrient pool, the organic nitrogen input by rivers accounts for only 23%. Nevertheless, there is a higher input of detritus into the sediment in the coastal box in terms of nitrogen, which results in a lower mass flow through the heterotrophic loop. Therefore, the nitrogen budget for the coastal box still shows a stronger dominance of the autotrophic loop than the phosphorus budget. As a consequence, the shift of the relative importance towards the heterotrophic loop is only achieved to the same degree as in the phosphorus budget for the offshore box near the central North Sea. Within the nitrogen budget the

effects of the different limitations acting can be highlighted even more by showing the different pathways for nitrate and ammonium. In the coastal box, with no severe nutrient limitation, the spring bloom is ended by increased grazing pressure of omnivorous mesozooplankton, which follows nearly parallel to the nitrate uptake in this box. In the offshore boxes the zooplankton grazing by omnivorous mesozooplankton follows the ammonium uptake, while the nutrient limitation stops the spring bloom in these boxes. This results in considerable differences in the uptake of nitrate and ammonium by diatoms and flagellates with increasing ammonium uptake with distance from the coast.

In the scenario runs, with different reductions of the river nutrient loads, the highest effects were observed in the coastal boxes with 14 to 15% difference in the net primary production in scenario B, representing a 50% reduction, and 21 to 30% in scenario C, representing a 75% reduction of the river loads. Overall, the influence is strongest in the continental coastal boxes and to a lesser degree in the neighbouring box to the north or the outflowing boxes, such as the Danish coastal and the Norwegian Trench box. This is in agreement with Klein and Van Buuren (1992), who argued that as a consequence of the current pattern, the discharges of the major rivers hardly affect the central North Sea.

As an effect of the reduction scenarios the simulated nutrient concentrations showed reduced winter and summer values compared to the standard run. However, the effect on the chlorophyll concentrations is rather low and only visible in a reduced standing stock in summer. The reason can be the silicate limitation during the spring peak, which has hardly changed by the reduction. As phosphate and nitrogen limitations begin to develop in summer because of the lower nutrient loads supplied by the rivers, the differences become obvious in the resulting chlorophyll concentration. Even though the overall uptake is reduced in the scenario run, the ammonium uptake by diatoms and flagellates has increased relative to the standard run. From the nitrogen budget, an increased activity of the heterotrophic loop in the coastal box appears in the reduction runs in relation to the overall lower nitrogen uptake. Therefore, the differences in the annual net primary production in the different river reduction scenarios and the standard run, can give only a slight indication of the changes occurring in the simulated ecosystem dynamics.

Furthermore, the differences in the annual net primary production are related to the forcing applied. While neglecting the atmospheric nitrogen input can cause differences in the primary production of up to 15%, neglecting for instance the particulate organic matter load causes only 10% difference. However, the major effects of neglecting the particulate organic matter appear in the continental coastal zone, where the river load scenarios also have highest effects and could therefore work additively.

Acknowledgements

This research was funded by the European Union under MAST contract number MAS2-CT92-0032-C. We are indebted to T. Pohlmann and W. Puls, who made their simulation results available for the use within ERSEM. We are particularly grateful to F. Hamberg and C. Kohlmeier for useful discussions during this work, the provision of the COCOA setup as well as the aggregation facility within the MOVIE visualisation environment. We wish to thank our colleagues W. Kühn, A. Moll and J. Pätsch for helpful discussions and comments. Valuable comments and criticism by J.G. Baretta-Bekker and J.W. Baretta led to many improvements of the manuscript. Thanks are also due to S. Gorr and A. Hufschmidt for their technical support.

References

Anonymous, 1992. Guidance document for the NSTF modelling workshop, 6–8 May, 1992, Den Haag, Directoraat Generaal Rijkswaterstaat, 41 pp.

Anonymous, 1995. North Sea Quality Status Report, Oslo and Paris Commissions, 132 pp.

Backhaus, J.O., 1985. A three-dimensional model for the simulation of shelf sea dynamics. Dt. Hydrogr. Z. 38, 167–262.

Backhaus, J., Hainbucher, D., 1987. A finite difference general circulation model for the shelf seas and its application to low frequency variability on the North European Shelf. In: Nihoul, J.C.J., Jamart, B.M. (Eds.), Three Dimensional Models of Marine and Estuarine Dynamics. Elsevier Oceanography Series 45, Amsterdam, pp. 221–244.

Baretta, J.W., Ebenhöh, W., Ruardij, P., 1995. An overview over the European Reginal Sea Ecosystem Model, a complex marine ecosystem model. Neth. J. Sea Res. 33, 233–246.

Baretta-Bekker, J.G., Baretta, J.W., Rasmussen, E.K., 1995. The

microbial food web in the European Regional Seas Ecosystem Model. Neth. J. Sea Res. 33, 363–379.

Baretta-Bekker, J.G., Baretta, J.W., Ebenhöh, W., 1997. Microbial dynamics in the marine ecosystem model ERSEM II with decoupled carbon assimilation and nutrient uptake J. Sea Res. 38, 195–211 (this issue).

Baretta-Bekker, J.G., Baretta, J.W., Hansen, A.S., Riemann, B., 1998. An improved model of carbon and nutrient dynamics in the microbial food web in marine ecosystems. Aquat. Microb. Ecol. 14, 91–108.

Beddig, S., Brockmann, U., Dannecker, W., Körner, D., Niemeier, U., Pohlmann, T., Puls, W., Radach, G., Rebers, A., Rick, H.-J, Schatzmann, M., Schlünzen H., Schulz, M., 1995. Nitrogen Fluxes in the German Bight ICES CM 1995/T:5, 21 pp.

Blackford, J.C., 1997. An analysis of benthic biological dynamics in a North Sea ecosystem model. J. Sea Res. 38, 213–230 (this issue).

Broekhuizen, N., McKenzie, E., 1995. Patterns of abundance for *Calanus* and smaller copepods in the North Sea: time series decomposition of two CPR data sets. Mar. Ecol. Prog. Ser. 118, 103–120.

Broekhuizen, N., Heath, M.R., Hay, S.J., Gurney, W.S., 1995. Modelling the dynamics of the North Sea's mesozooplankton. Neth. J. Sea Res. 33, 381–406.

Ebenhöh, W., Baretta-Bekker, J.G., Baretta, J.W., 1997. The primary production module in the marine ecosystem model ERSEM II with emphasis on the light forcing. J. Sea Res. 38, 173–193 (this issue).

Howarth, M.J., Dyer, K.R., Joint, I.R., Hydes, D.J., Purdie, D.A., Edmunds, H., Jones, J.E., Lowry, R.K., Moffat, T.J., Pomroy, A.J., Proctor, R., 1994. Seasonal cycles and their spatial variability. In: Charnock, H., Dyer, K.R., Huthnance, J.M., Liss, P.S., Simpsom, J.H., Tett, P.B. (Eds.), Understanding the North Sea System. The Royal Society, Chapman and Hall, London, pp. 5–25.

ICES, 1983. Flushing times of the North Sea. Coop. Res. Rep. Int. Counc. Explor. Mer 123, 159 pp.

Joint, I., Pomroy, A., 1993. Phytoplankton biomass and production in the southern North Sea. Mar. Ecol. Prog. Ser. 99, 169–182.

Klein, A.O.W., Van Buuren, J.T., 1992. Eutrophication of the North Sea in Dutch coastal zone 1976–1990. Ministry of Transport and Public Works, Tidal Waters Division, Report WS-92.003, The Hague, 70 pp.

Lenhart, H.J., Pohlmann, T., 1997. The ICES box approach in relation to results of a North Sea circulation model. Tellus 49A, 139–160.

Lenhart, H.J., Radach, G., Backhaus, J.O., Pohlmann, T., 1995. Simulations of the North Sea circulation, its variability, and its implementation as hydrodynamical forcing in ERSEM. Neth. J. Sea Res. 33, 271–299.

Lenhart, H.J., Pätsch, J., Radach, G., 1996. Daily nutrient loads for the European continental rivers during 1977–1993. Discharges and loads of rivers entering the North Sea. ZMK Ber. 22, 159 pp.

Moll, A., 1995. Regionale Differenzierung der Primärproduktion in der Nordsee: Untersuchungen mit einem drei-dimensionalen Modell. ZMK Ber. 19, 151 pp.

Moll, A., 1997. Modeling primary production in the North Sea. Oceanography 10, 24–26.

Pätsch, J., 1994. MOCADOB a model generating synthetical time series of solar radiation for the North Sea. ZMK Technical Report 16, 67 pp.

Pätsch, J., 1997. Auswirkungen anhaltender Eutrophierung der Nordsee: Langzeituntersuchungen mit dem Ökosystemmodell ERSEM. Dissertation Uni. Hamburg, 171 pp.

Pätsch, J., Radach, G., 1997. Long-term simulation of the eutrophication of the North Sea: temporal development of nutrients, chlorophyll and primary production in comparison to observations. J. Sea Res. 275–310 (this issue).

Peeters, J.C.H., Peperzak, L., 1990. Nutrient limitation in the North Sea: a biomass approach. Neth. J. Sea Res. 26, 61–73.

Pohlmann, T., 1991. Untersuchung hydro- und thermodynamischer Prozesse in der Nordsee mit einem dreidimensionalen numerischen Modell. Dissertation Uni. Hamburg, 116 pp.

Pohlmann, T., 1996a. Predicting the thermocline in a circulation model of the North Sea. Part I: Model description, calibration, and verification. Cont. Shelf Res. 7, 131–146.

Pohlmann, T., 1996b. Calculating the annual cycle of the vertical eddy viscosity in the North Sea with a three dimensional baroclinic shelf sea circulation model. Cont. Shelf Res. 7, 147–162.

Pohlmann, T., Puls, W., 1994. Currents and transport in water. In: Sündermann, J. (Ed.), Circulation and Contaminant Fluxes in the North Sea. Springer Verlag, Berlin, pp. 345–402.

Puls, W., Sündermann, J., 1990. Simulation of suspended sediment dispersion in the North Sea. In: Cheng, R.T. (Ed.), Residual Currents and Long-term Transport. Coast. Estuar. Stud. 38, 356–372.

Radach, G., Lenhart, H.J., 1995. Nutrient dynamics in the North Sea: Fluxes and budgets in the water derived from ERSEM. Neth. J. Sea Res. 33, 301–335.

Radach, G., Pätsch, J., 1997. Climatological annual cycles of nutrients and chlorophyll in the North. Sea. J. Sea Res. 38, 231–248 (this issue).

Radach, G., Pätsch, J., Gekeler, J., Herbig, K., 1996. Horizontal distribution of annual cycles of nutrients and chlorophyll in time in the North Sea. Validation data sets for the ERSEM setups ND15, ND130 and COCOA. ZMK Ber. 20, 172 pp.

Reid, P.C., Taylor, A.H., Stephens, J.A., 1988. The hydrography and hydrographic balances of the North Sea. In: Salomons, W., Bayne, B.L., Duursma, E.K., Förster, U. (Eds.), Pollution of the North Sea, An Assessment. Springer Verlag, Heidelberg, pp. 3–19.

Rendell, A.R., Ottley, J.O., Jickells, T.D., Harrison, R.M., 1993. The atmospheric input of nitrogen species to the North Sea. Tellus 45B, 53–63.

Ruardij, P., Van Raaphorst, W., 1995. Benthic nutrient regeneration in the ERSEM ecosystem model of North Sea. Neth. J. Sea Res. 33, 435–483.

Simpson, J.H., Hughes, D.H., Morris, N.C.G., 1977. The relation of the seasonal stratification to tidal mixing on the continental shelf. In: Angel, M.V. (Ed.), A Voyage of Discovery: George

Deacon 70th Anniversary Volume. Pergamon, London, pp. 327–340.

Skogen, M.D., Svendsen, E., Berntsen, J., Asknes, D., Ulvestad, K.B., 1995. Modelling the primary production in the North Sea using a coupled three-dimensional physical–chemical–biological ocean model. Estuar. Coast. Shelf Sci. 41, 545–565.

Van Bennekom, A.J., Gieskes, W.W.C., Tijssen, S.B., 1975. Eutrophication of Dutch coastal waters. Proc. R. Soc. B 189, 359–374.

Van Beusekom, J., Diel-Christiansen, S., 1994. A synthesis of phyto- and zooplankton dynamics in the North Sea environment. Godalming: WWF-World Wide Fund for Nature, 148 pp.

Varela, R.A., Cruzado, A., Gabaldón, J.E., 1995. Modelling primary production in the North Sea using the European Regional Seas Ecosystem Model. Neth. J. Sea Res. 33, 337–361.